

# Estimation of the Order of Non-Parametric Hidden Markov Models using the Singular Values of an Integral Operator

Marie Du Roy de Chaumaray, Salima El Kolei and Matthieu Marbac  
Univ. Rennes, Ensaï, CNRS, CREST - UMR 9194, F-35000 Rennes, France

October 10, 2022

## Abstract

We are interested in assessing the order of a finite-state Hidden Markov Model (HMM) with the only two assumptions that the transition matrix of the latent Markov chain has full rank and that the density functions of the emission distributions are linearly independent. We introduce a new procedure for estimating this order by investigating the rank of some well-chosen integral operator which relies on the distribution of a pair of consecutive observations. This method circumvents the usual limits of the spectral method when it is used for estimating the order of an HMM: it avoids the choice of the basis functions; it does not require any knowledge of an upper-bound on the order of the HMM (for the spectral method, such an upper-bound is defined by the number of basis functions); it permits to easily handle different types of data (including continuous data, circular data or multivariate continuous data) with a suitable choice of kernel. The method relies on the fact that the order of the HMM can be identified from the distribution of a pair of consecutive observations and that this order is equal to the rank of some integral operator (*i.e.* the number of its singular values that are non-zero). Since only the empirical counter-part of the singular values of the operator can be obtained, we propose a data-driven thresholding procedure. An upper-bound on the probability of overestimating the order of the HMM is established. Moreover, sufficient conditions on the bandwidth used for kernel density estimation and on the threshold are stated to obtain the consistency of the estimator of the order of the HMM. The procedure is easily implemented since the values of all the tuning parameters are determined by the sample size. We illustrate the relevance of our approach by numerical experiments on simulated and benchmark data, including continuous data but also multivariate data or directional data.

*Keywords:* Hidden Markov models; Latent state model; Model selection; Non-parametric estimation;

# 1 Introduction

A discrete-time homogeneous hidden Markov model (HMM) defines the distribution of an observed process  $(\mathbf{Y}_t)_{t \in \mathbb{N}}$  and a latent process  $(X_t)_{t \in \mathbb{N}}$  such that the unobserved states  $X_t$  follows a Markov chain, the  $\mathbf{Y}_t$  are independent given the  $X_t$  and their conditional distributions, called emission distributions, only depend on the current state  $X_t$ . This paper focuses on finite state HMMs where the latent process has finite state space  $\{1, \dots, L\}$ , the integer  $L$  being called the order of the HMM. In this framework, the model is completely described by the order  $L$ , the initial distribution and the transition matrix of the hidden chain, and the emission distributions. Since the marginal distribution of each  $\mathbf{Y}_t$  is a finite mixture model, finite state HMMs can be seen as an extension of finite mixture models where the assumption of independence between observations is relaxed (*i.e.*,  $\mathbf{Y}_t$  and  $\mathbf{Y}_{t'}$  are not independent). HMMs are a popular tool for modeling the dependency structure for univariate and multivariate processes driven by a latent Markov chain (see Juang and Rabiner (1991); Yang et al. (1995); Krogh et al. (2001); Choo et al. (2004); Zucchini and MacDonald (2009) for examples of applications). They also provide tractable models for circular time series widely used in biology, meteorology and climate applications to model for instance the speed and the direction of wind, ocean current, or animal movements (see Holzmann et al. (2006); Bulla et al. (2012); Mastrantonio and Calise (2016)). Inferring the right order of the latent chain is an important issue, which precedes the estimation the model parameters and their interpretation in the context of the modeling of some phenomenon.

This paper focuses on the estimation of the order  $L$  from univariate and multivariate data  $(\mathbf{Y}_t)_{t \in \mathbb{N}}$  in a non-parametric setting. The estimation of  $L$  is indeed achieved without any parametric assumption on the emission distributions, since we only require the linear independence between their density functions.

Initial developments on HMMs have been made in a parametric framework, which considers that the emission distributions belong to some given parametric distribution family. Considering the order of the HMM as known, the existing literature provides the parameter identifiability (Petrie, 1969), the algorithm for assessing the maximum likelihood estimator

(MLE; Baum et al. (1970)), the consistency of the MLE (Leroux, 1992) and its asymptotic normality (Bickel et al., 1998). The identification of the order is more challenging and represents a difficult task, mainly because of a loss of identifiability of the model parameters when the order is overestimated. The standard assumptions used to control the likelihood ratio test statistics, are thus not satisfied when the order is overestimated. For instance, Gassiat and Keribin (2000) show that this statistic can diverge even for bounded parameters. Note that this issue already appears when estimating the number of components in parametric finite mixture models (Ciuperca, 2002). Therefore, homogeneous tests can be built by extending the homogeneous tests based on quasi-likelihood and developed under the independence assumption (Holzmann and Schwaiger, 2016). General order estimation can be achieved by penalized likelihood approaches (Volant et al., 2014) or cross-validation approaches (Celeux and Durand, 2008). Using tools from information theory, Gassiat and Boucheron (2003) have shown the strong consistency of the estimator of the order obtained by penalized maximum likelihood. Moreover, Bayesian approaches can be used by penalizing the likelihood and thus avoiding the issues due to the lack of identifiability of the parameters when the order is overestimated (Gassiat and Rousseau, 2014). Alternatively, Robert et al. (2000) propose a Bayesian inference of the order  $L$  through a reversible jump Markov Chain Monte Carlo method (MCMC). In Chopin (2007), the author also proposes a Bayesian strategy based on sequential Monte Carlo filter and MCMC. However, all these approaches consider parametric emission distributions but it is not always possible to restrict the model to such a convenient finite-dimensional space. Moreover they provide biased results when their parametric assumptions are violated. In such cases, non-parametric approaches can be used to model the emission distributions.

Non-parametric HMMs have been proved to be useful in a wide range of applications (see Zhao (2011) for financial applications, Couvreur and Couvreur (2000) for voice activity detection, Lambert et al. (2003) for climate state identification and Yau et al. (2011) for genomic applications). Nevertheless, identifiability of the parameters of finite state HMMs with non-parametric emission distributions has been investigated recently. Gassiat and Rousseau

(2016) consider the case of translation HMMs. They show that all the model parameters (including the infinite dimensional parameters) are identifiable as soon as the matrix that defines the joint distribution of two consecutive latent variables, is non-singular and the translation parameters are distinct. Note that their conditions are weaker than those used to obtain identifiability for location-scale mixture models. Indeed, for the latter, constraints must be added such as considering symmetric distributions (Hunter et al., 2007). This additional assumption is no longer required for translation HMMs because of the dependency between a pair of consecutive observations. Based on the results of parameter identifiability for a mixture of products of univariate distributions (Allman et al., 2009), Gassiat et al. (2016) state weaker sufficient conditions for parameter identifiability since they consider a full rank transition matrix of the latent chain and linearly independent emission probability distributions. The method introduced by the present paper for estimating the order of an HMM, is developed under these assumptions. Note that the assumptions made on the emission distributions have been weakened again by Alexandrovich et al. (2016) since they only require that the emission distributions are different.

To estimate the (finite and infinite dimensional) parameters of non-parametric HMMs, kernel-based (Bonhomme et al., 2016a) or wavelet-based (Jin and Mokhtarian, 2006) approaches can be used. However, these approaches consider an EM-like algorithm which does not have the ascendent property (Benaglia et al., 2009). Moreover, kernel-based approaches can also be used to maximize a smoothed version of the pseudo-likelihood (*i.e.*, likelihood function based on the distribution of few consecutive observations) by using a Majorization-Minimization algorithm (Levine et al., 2011). Alternatively, Bonhomme et al. (2016a) and De Castro et al. (2017) extended the spectral method proposed by Hsu et al. (2012) for estimating parametric HMMs, in order to deal with a non-parametric framework. However, all these methods are developed for a known order of the HMM. Note that spectral methods have been used to estimate the number of components of mixture models based on independent observations. Indeed, in the Section 5 of Supplementary material of Bonhomme et al. (2016b) a rank-based procedure using the approach of Kleibergen and Paap (2006) is

proposed to estimate the number of components. Thus, this result generalizes the approach of Kasahara and Shimotsu (2014) by allowing other types of approximating functions than the discretization (*e.g.* Jacobi or Hermite polynomials) to apply spectral approaches for estimating the number of components.

Estimating the order of a non-parametric HMM is still a challenging problem and to the best of our knowledge Lehéricy (2019) is the only paper to consider this problem in this non-parametric setting. The author proposes two methods that provide strongly consistent estimators of the order of the HMM. The first method considers a minimization of a penalized least-square criterion that relies on a projection of the emission distributions onto a family of nested parametric subspaces. For each subspace and each number of latent states, the criterion used for model selection is computed by minimizing the empirical counterpart of the penalized  $L^2$  distance. Thus, the method provides an estimator of the order of the HMM together with estimators of the emission distributions. The second method uses an estimator of the rank of some matrix computed from the distribution of a pair of consecutive observations. More precisely, this method relies on a spectral approach applied on the matrix containing the coordinates of the density of a pair of consecutive observations in some orthonormal basis. Thus, this method could be seen as an extension of the spectral method described in the Section 5 of Supplementary material of Bonhomme et al. (2016b) to HMM. These two methods are complementary in practice. Indeed, numerical experiments presented in Lehéricy (2019) show that the penalized least-square method is more efficient for moderate sample sizes. Indeed, the non-convex criterion raises many problems for the minimization, in practice. To overcome this difficulty, the author proposes to use an approximate minimization algorithm (see Hansen and Auger (2011)) that requires a good initial condition since it might otherwise remain trapped in a local minima which renders this approach time-consuming for multivariate data and large sample. Furthermore, considering all the subspaces and all the possible numbers of latent states makes this method computationally greedy. Therefore, the spectral method should be considered for large sample sizes. Both methods involve a tuning parameter (*i.e.*, constant in the penalty term of the penalized criterion and threshold for

the spectral method) but also choices of the subspaces (*i.e.*, family of nested parametric subspaces or the orthonormal basis) that can highly impact the results (see our numerical experiments).

The present paper introduces a simple method for selecting the order of a non-parametric HMM. This approach is based on the methodology of Kwon and Mbakop (2021) where the authors propose a consistent estimator of the order in non-parametric mixture models by counting the non-zero singular values of some well-chosen integral operator after applying a data-driven thresholding rule. We propose to adapt the construction of the integral operator to the structure of a HMM and thus obtain a method for selecting the order of the hidden Markov chain. The interest of this approach lies in the fact that unlike most spectral methods like in Bonhomme et al. (2016a); De Castro et al. (2017); Lehéricy (2019) based on noisy matrices, the method does not require any choices of a functional basis or its number of elements. Moreover, a simple thresholding rule is established to obtain a consistent estimator of the order. Note that in Lehéricy (2019) the model selection for the spectral method is also based on a thresholding rule of the singular values whose choice is a delicate issue since it depends on the functional basis and on the number of elements. In Lehéricy (2019), an empirical method based on slope heuristic is proposed for the practical application. However, this approach requires an additional tuning parameter that states the number of singular values used to apply the slope heuristic. In theory, for the spectral methods to work, the rank of the spectral matrix needs to be equal to the order of the chain. Thus, it is necessary that the number of elements of the orthonormal basis tends to infinity, otherwise we only obtain an estimator of an upper-bound of the order. However, defining the thresholding rule for the case of increasing number of basis elements is still an open problem for the spectral methods. Indeed, for instance, the rank study performed in Kleibergen and Paap (2006) should be extended to matrices with increasing dimension (but fixed rank). Thus, in practice, the number of basis elements is set a priori. This number corresponds to an upper-bound on the order of the HMM. To the best of our knowledge, since the proposed method avoids the use of functional basis, it is the first method which does not make assumptions

on a upper-bound of the order to be estimated.

In this paper, the construction of the integral operator is built from kernel density estimation which allows this methodology to be considered for various applications implying different types of data including univariate, multivariate or circular data. To state the consistency of the estimator, the present paper contains different steps, each having its own contribution. We first show that the order of the HMM can be assessed from the distribution of a couple of consecutive observations without having to consider any functional basis (thus avoiding the issue of its choice), under standard assumptions (*i.e.*, full rank transition matrix of the latent Markov chain and linear independence between the emission distribution functions). We then show that this order is equal to the number of non-zero singular values of some integral operator, which will be detailed later on. Since only an empirical version of this operator can be obtained, like for any model selection, a thresholding rule is needed to estimate the order. Indeed, despite the fact that the rank of the theoretical operator is equal to the order of the HMM, the rank of its empirical counter-part is generally larger. Thus, we propose an extension of the thresholding rule of Kwon and Mbakop (2021) to the case of HMM. We present an upper-bound of the probability of overestimating the order of the HMM computed from finite samples. Moreover, we establish the consistency of the estimator of the order of the HMM. Since the threshold rule depends on the bandwidth of the kernel, we show that the proposed approach only requires choosing the value of the bandwidth. Moreover, we provide a range for the bandwidth that only depends on the sample size and which ensures the consistency of the approach. Thus, the procedure is easily implemented since the values of all the tuning parameters are determined by the sample size

This paper is organized as follows. Section 2 shows that the order of the HMM is equal to the rank of a specific integral operator. Section 3 explains how the singular values of the operator can be computed in practice and presents the estimator of the order. Section 4 presents the finite-sample size and the asymptotic properties of the estimator (including its consistency). Section 5 illustrates the consistency of the estimator on simulated data and shows the relevance of the proposed method on benchmark data (including circular data).

Section 6 gives a conclusion.

## 2 Rank of integral operators and HMM order

### 2.1 Hidden Markov model

Let  $\mathbf{Y} = (\mathbf{Y}_1^\top, \dots, \mathbf{Y}_{n+1}^\top)^\top$  be a stationary sequence of random vectors  $\mathbf{Y}_t$ , where  $\mathbf{Y}_t \in \mathbb{R}^d$  follows a finite state hidden Markov model (HMM) with  $L$  latent states. This model assumes that there exists a stationary Markov chain  $\mathbf{X} = (X_1, \dots, X_{n+1})^\top$  that is unobserved, where  $X_t \in \{1, \dots, L\}$ . Moreover, conditionally on  $\mathbf{X}$ , the  $\mathbf{Y}_t$ 's are independent and their distribution only depends on the current state  $X_t$ . The Markov chain is defined by a full rank transition matrix  $\mathbf{A}$  having  $\boldsymbol{\pi} = (\pi_1, \dots, \pi_L)^\top$  as stationary distribution. Finally, the densities of the emission distributions  $f_1, \dots, f_L$  are assumed to be linearly independent, where  $f_\ell$  defines the conditional distribution of  $\mathbf{Y}_t$  given  $X_t = \ell$ . The density of  $\mathbf{y}$  is defined by

$$p(\mathbf{y}) = \sum_{\mathbf{x} \in \{1, \dots, L\}^{n+1}} \pi_{x_1} f_{x_1}(\mathbf{y}_1) \prod_{t=1}^n A[x_t, x_{t+1}] f_{x_{t+1}}(\mathbf{y}_{t+1}). \quad (1)$$

The conditions made on the transition matrix and on the emission distributions are stated by the following set of assumptions. Note that these assumptions are mild and have been considered already in Gassiat et al. (2016) to obtain the identifiability of an HMM based on the distribution of three consecutive observations. Moreover, the stationarity and ergodicity Assumption 1.1 is completely standard in order to obtain convergence results in this context (see for example De Castro et al. (2016, 2017)).

**Assumption 1.**

1. *The transition matrix  $\mathbf{A}$  has full rank, is irreducible and aperiodic with stationary distribution  $\boldsymbol{\pi} = (\pi_1, \dots, \pi_L)^\top$ .*
2. *The densities defining the emission distributions  $\{f_\ell\}_{\ell=1}^L$  are linearly independent (i.e., if  $\boldsymbol{\xi} = (\xi_1, \dots, \xi_L) \in \mathbb{R}^L$  is such that for any  $\mathbf{z} \in \mathbb{R}^d$ ,  $\sum_{\ell=1}^L \xi_\ell f_\ell(\mathbf{z}) = 0$  then  $\boldsymbol{\xi} = \mathbf{0}$ ) and are square integrable on  $\mathbb{R}^d$ .*

Identifiability of an HMM can be obtained from the distribution of three consecutive observations (Gassiat et al., 2016) or from the distribution of a pair of consecutive observations when the emission distribution are defined as translations of the same distribution (Gassiat and Rousseau, 2016). From (1), the distribution of a pair of consecutive observations  $(\mathbf{Y}_t^\top, \mathbf{Y}_{t+1}^\top)^\top$  is defined by the density

$$p(\mathbf{y}_t, \mathbf{y}_{t+1}) = \sum_{\ell=1}^L \pi_\ell f_\ell(\mathbf{y}_t) g_\ell(\mathbf{y}_{t+1}), \quad (2)$$

where  $g_\ell$  is the density of  $\mathbf{Y}_{t+1}$  given  $X_t = \ell$  and is defined by

$$g_\ell(\mathbf{y}_{t+1}) = \sum_{m=1}^L A[\ell, m] f_m(\mathbf{y}_{t+1}). \quad (3)$$

The aim is to make inference on the order  $L$ . This can be achieved by using the distribution of a pair of consecutive observations. Indeed, the following lemma shows that the order of the HMM can be identified from the distribution of a pair of consecutive observations.

**Lemma 1.** *If Assumption 1 holds true, then  $L$  is identifiable from the distribution of a pair of consecutive observations defined by (2).*

Note that (2) is a mixture model where the density of each of the  $L$  components is defined as a product of two specific densities. Moreover, the mixture proportions correspond to the probabilities of latent states defined by the stationary distribution of the Markov chain. Note that Assumption 1.2 corresponds to the assumption stated by Kwon and Mbakop (2021) for obtaining the identifiability of a mixture model defined as a product of univariate densities (see also Allman et al. (2009) and Kasahara and Shimotsu (2014)). Hence, estimating the number of latent states is equivalent to estimating the number of components in (2). Thus, we can extend to HMMs the approach of Kwon and Mbakop (2021) for estimating the number of components in a nonparametric mixture model. Note that one main difference between the HMM framework and the framework of Kwon and Mbakop (2021) is that we have to take into account the dependencies between the observations  $\mathbf{y}_t$  while the approach of Kwon and Mbakop (2021) considers a sample composed of independent observations. Moreover, in

our case, the second density of any component (*i.e.*,  $g_\ell$ ) is a convex combination of the first densities of all the components (*i.e.*,  $f_1, \dots, f_L$ ), while  $g_\ell$  and  $f_\ell$  are not related in Kwon and Mbakop (2021).

## 2.2 Integral operator and distribution of pairs of successive observations

One way to achieve model selection for non-parametric mixture models is to discretize the data into bins. However, for a fixed number of bins, the resulting estimator only provides a lower bound of the number of components (Kasahara and Shimotsu, 2014). Moreover, if consistency is wanted, then the number of bins should tend to infinity as the sample size tends to infinity, at an appropriate rate (Du Roy de Chaumaray and Marbac, 2021). However, the way the data are discretized can impact the results, in particular for small samples. To overcome this problem, a more general approach, based on integral operators, is proposed by Kwon and Mbakop (2021). We extend this approach to the HMM model defined by (1)-(3). Let  $L^2(\mathbb{R}^d)$  be the Hilbert space of square integrable functions on  $\mathbb{R}^d$ . We consider the integral operator  $T : L^2(\mathbb{R}^d) \rightarrow L^2(\mathbb{R}^d)$  defined, for any function  $\omega \in L^2(\mathbb{R}^d)$ , by

$$[T(\omega)](\mathbf{z}_2) = \int_{\mathbb{R}^d} \omega(\mathbf{z}_1) p(\mathbf{z}_1, \mathbf{z}_2) d\mathbf{z}_1,$$

where  $p$  is the joint distribution given in Equation 2. Thus, if we denote by  $g_\ell \otimes f_\ell$  the tensor product defined by  $g_\ell \otimes f_\ell : L^2(\mathbb{R}^d) \rightarrow L^2(\mathbb{R}^d)$  with  $g_\ell \otimes f_\ell(\omega) = g_\ell < f_\ell, \omega >$  and  $< f_\ell, \omega > = \int_{\mathbb{R}^d} \omega(\mathbf{z}_1) f_\ell(\mathbf{z}_1) d\mathbf{z}_1$ , then the operator can be represented by

$$T = \sum_{\ell=1}^L \pi_\ell g_\ell \otimes f_\ell.$$

Under Assumption 1, a direct consequence of Lemma 1 (see Proposition 2.1 in Kwon and Mbakop (2021)) implies that

$$\text{rank}(T) = L.$$

where  $\text{rank}(T)$  is defined as the dimension of the operator  $T$ . Thus, the operator  $T$  is compact and admits a singular value decomposition based on  $L$  non-zero singular values

$\sigma_1(T) \geq \dots \geq \sigma_L(T) > 0$ , where  $\sigma_j(T)$  denotes the  $j$ -th largest singular value of operator  $T$ . Therefore, estimating the number of latent states  $L$  can be achieved by estimating the number of non-zero singular values of  $T$ .

### 2.3 Smoothed integral operator

From the observed sample  $\mathbf{y}$ , controlling the accuracy of the estimators of the singular values of  $T$  is a delicate task. Therefore, we introduce a smoothed version of the integral operator, denoted by  $T_h$ , for which we will be able to compute unbiased estimators of its singular values (see Section 3). The operator  $T_h : L^2(\mathbb{R}^d) \rightarrow L^2(\mathbb{R}^d)$  is defined, for any function  $\omega \in L^2(\mathbb{R}^d)$ , by

$$[T_h(\omega)](\mathbf{z}_2) = \int_{\mathbb{R}^d} \omega(\mathbf{z}_1) p_h(\mathbf{z}_1, \mathbf{z}_2) d\mathbf{z}_1,$$

where  $p_h$  is the function obtained by the convolution between the density  $p$  of a pair of consecutive observations given in (2) and a multivariate kernel defined as a product of univariate kernels  $K$ , as follows,

$$p_h(\mathbf{z}_1, \mathbf{z}_2) = \int_{\mathbb{R}^d \times \mathbb{R}^d} p(\mathbf{y}_1, \mathbf{y}_2) K_h^d(\mathbf{z}_1 - \mathbf{y}_1) K_h^d(\mathbf{z}_2 - \mathbf{y}_2) d\mathbf{y}_1 d\mathbf{y}_2,$$

where  $\mathbf{z}_1 \in \mathbb{R}^d$ ,  $\mathbf{z}_2 \in \mathbb{R}^d$ ,  $K_h^d(\mathbf{u}) = \prod_{j=1}^d K(u_j/h)/h$ ,  $\mathbf{u} = (u_1, \dots, u_d)^\top \in \mathbb{R}^d$ ,  $K$  being an univariate kernel and  $h > 0$  being a bandwidth. The following conditions on the kernel will allow the links between  $T$  and  $T_h$  to be quantified. Note that these assumptions are not restrictive since the kernel is chosen by the user and many well-known kernels satisfy those conditions.

**Assumption 2.** 1. *The kernel  $K$  has a non-vanishing Fourier transform.*

2. *The kernel  $K$  belongs on  $L^1(\mathbb{R}^d) \cap L^2(\mathbb{R}^d)$ .*

3. *The kernel  $K$  satisfies  $\int u K(u) du = 0$  and  $0 < \int u^2 K(u) du < \infty$ .*

Under Assumptions 1 and 2, as a direct consequence of Proposition 2.2 in Kwon and Mbakop (2021), we have

$$\text{rank}(T_h) = L. \tag{4}$$

Therefore, for any  $j \in \{1, \dots, L\}$ , we have  $\sigma_j(T_h) > 0$  and for any  $j > L$ , we have  $\sigma_j(T_h) = 0$ . To control the differences between the non-zero singular values of  $T$  and  $T_h$  respectively, we introduce regularity conditions on the density of a pair of consecutive observations, which are stated by the following assumption.

**Assumption 3.** *The density function  $p$  has partial derivatives at least until order 3 that belongs to  $L^1(\mathbb{R}^d) \cap L^2(\mathbb{R}^d)$ .*

Note that Assumption 3 is equivalent to requiring that the emission density functions are  $C^3$  and belong to  $L^1(\mathbb{R}^d) \cap L^2(\mathbb{R}^d)$ . The following lemma give an upper bound to the difference between the non-zero singular values of  $T$  and  $T_h$ . Thus, it allows us to investigate the impact of the smoothing on the singular value decomposition outputs.

**Lemma 2.** *Under Assumptions 1, 2 and 3, we have*

$$\sum_{\ell=1}^L (\sigma_\ell(T) - \sigma_\ell(T_h))^2 = O(h^4).$$

In summary, Equation (4) shows that  $T$  and  $T_h$  have the same number of non-zero singular values. In addition, Lemma 2 allows us to control the bias induced by the approximation of the non-zero singular values  $\sigma_\ell(T)$  by the  $\sigma_\ell(T_h)$ , for each  $\ell = 1, \dots, L$  and for any bandwidth  $h$ . In the next section, we show how to obtain unbiased estimators of  $\sigma_\ell(T_h)$  for each  $\ell = 1, \dots, L$ . After describing the estimators of the singular values of  $T_h$ , a thresholding rule is presented in order to take the variance of those estimators into account.

### 3 Estimation

The estimation of the order of the HMM relies on the singular value decomposition of the operator  $T_h$ , and more precisely, of its empirical counter-part based on the observations. However, performing this decomposition is not straightforward in general. Thus, we will relate them to the singular value decomposition of some well-chosen matrix. This section presents an empirical matrix that has the same singular values as the empirical counter-part of  $T_h$ , and thus permits to circumvent the difficult task of performing the singular

value decomposition of the empirical counter-part of  $T_h$ . Then, this section presents the thresholding rule that is applied on these singular values to compute the estimator of the HMM order.

### 3.1 Estimating the smoothed integral operator

From the observed sample  $\mathbf{y}$ , we can compute the unbiased estimator of  $p_h$  denoted by  $\hat{p}_{h,\mathbf{y}}$  defined for any  $\mathbf{z}_1 \in \mathbb{R}^d$  and  $\mathbf{z}_2 \in \mathbb{R}^d$  by

$$\hat{p}_{h,\mathbf{y}}(\mathbf{z}_1, \mathbf{z}_2) = \frac{1}{n} \sum_{t=1}^n K_h^d(\mathbf{z}_1 - \mathbf{y}_t) K_h^d(\mathbf{z}_2 - \mathbf{y}_{t+1}). \quad (5)$$

Thus, we can deduce the empirical version of the smoothed operator  $\hat{T}_{h,\mathbf{y}}$  defined by

$$[\hat{T}_{h,\mathbf{y}}(\omega)](\mathbf{z}_2) = \int \omega(\mathbf{z}_1) \hat{p}_{h,\mathbf{y}}(\mathbf{z}_1, \mathbf{z}_2) d\mathbf{z}_1.$$

To estimate the rank of  $T_h$ , it suffices to estimate the singular values of  $T_h$  by considering a singular value decomposition of  $\hat{T}_{h,\mathbf{y}}$ . However, performing the singular value decomposition of an operator directly is not straightforward. Therefore, we introduce a  $n \times n$  matrix  $\hat{\mathbf{V}}_{h,\mathbf{y}}$  that has the same singular values as  $\hat{T}_{h,\mathbf{y}}$ . Let the empirical  $n \times n$  matrix  $\hat{\mathbf{V}}_{h,\mathbf{y}}$  be defined by

$$\hat{\mathbf{V}}_{h,\mathbf{y}} = \frac{1}{n} \Delta_1^\top \hat{\mathbf{W}}_{h,\mathbf{y}}^{1/2} \Delta_1 \Delta_{n+1}^\top \hat{\mathbf{W}}_{h,\mathbf{y}}^{1/2} \Delta_{n+1}, \quad (6)$$

where  $\Delta_1$  and  $\Delta_{n+1}$  are the  $(n+1) \times n$  matrices defined as block matrices by  $\Delta_1^\top = [\mathbf{0}_n \ \mathbf{I}_n]$  and  $\Delta_{n+1}^\top = [\mathbf{I}_n \ \mathbf{0}_n]$ , where  $\mathbf{I}_n$  is the identity matrix of size  $n \times n$  and  $\mathbf{0}_n$  is the null vector of length  $n$ , and where  $\hat{\mathbf{W}}_{h,\mathbf{y}}$  is the  $(n+1) \times (n+1)$  matrix defined by  $\hat{\mathbf{W}}_{h,\mathbf{y}}[t, s] = \phi_h(\mathbf{y}_t, \mathbf{y}_s)$ , for  $1 \leq t, s \leq (n+1)$  where the function  $\phi_h$  is such that  $\phi_h : \mathbb{R}^{2d} \rightarrow \mathbb{R}$  and

$$\phi_h(\mathbf{y}_t, \mathbf{y}_s) = \int_{\mathbb{R}^d} K_h^d(\mathbf{z}_1 - \mathbf{y}_t) K_h^d(\mathbf{z}_1 - \mathbf{y}_s) d\mathbf{z}_1,$$

where  $h > 0$  is a bandwidth and  $K^d$  is a  $d$ -dimensional kernel. The following lemma shows that the singular values of  $\hat{\mathbf{V}}_{h,\mathbf{y}}$  are equal to the singular values of  $\hat{T}_{h,\mathbf{y}}$ .

**Lemma 3.** *If Assumptions 1 and 2 hold true, then the singular values of  $\hat{\mathbf{V}}_{h,\mathbf{y}}$  and  $\hat{T}_{h,\mathbf{y}}$  are equal, meaning that for any  $j = 1, \dots, n$ , we have*

$$\sigma_j(\hat{\mathbf{V}}_{h,\mathbf{y}}) = \sigma_j(\hat{T}_{h,\mathbf{y}}).$$

### 3.2 Estimating the number of latent states

Since we are able to compute the singular values of the empirical version of the smoothed operators  $\hat{T}_{h,y}$ , we can use them to estimate the number of latent states  $L$ . However, the rank of  $\hat{T}_{h,y}$  is not equal to  $L$ , since in general, the number of non-zero singular values of such an operator is  $n$ . Therefore, we need to apply a threshold  $\tau > 0$  on  $\sigma_1(\hat{T}_{h,y}), \dots, \sigma_n(\hat{T}_{h,y})$  to build the estimator  $\hat{L}(\tau, h)$ . This estimator of the number of latent states  $\hat{L}$  is defined by

$$\hat{L}(\tau, h) = \text{card} \left( \left\{ \ell : r_\ell(\hat{T}_{h,y}) > \tau \right\} \right), \quad (7)$$

where for any operator  $\mathcal{T}$  we have

$$r_\ell(\mathcal{T}) = \left[ \sum_{j=\ell}^n \sigma_j^2(\mathcal{T}) \right]^{1/2}. \quad (8)$$

Note that the estimator of the order defined by (7) depends on two tuning parameters: the threshold  $\tau$  and the bandwidth  $h$ . The next section shows that the threshold is related to the probability of overestimating  $L$ . Moreover, it shows that consistency can be achieved by relating  $\tau$  and  $h$  with the sample size, and thus a data-driven procedure can be obtained.

## 4 Properties of the estimator of the HMM order

This section is devoted to the study of the estimator  $\hat{L}(\tau, h)$ . First, a non-asymptotic control of the estimator is stated. An asymptotic control of the estimator leading to its consistency is then presented.

### 4.1 Non-asymptotic results

The following theorem gives an upper-bound on the probability of overestimating the number of latent states when this number is estimated by  $\hat{L}(\tau, h)$ . This result is stated by controlling  $\|\hat{T}_{h,y} - T_h\|_{L^2(\mathbb{R}^d)}$  via a concentration inequality. This control is achieved under mild assumptions (Assumptions 1 and 2) because it only requires that  $\text{rank}(T) = \text{rank}(T_h) = L$ . The second part of the theorem shows that, under additional conditions, the number of

latent states is not underestimated. Thus, we obtain a lower-bound on the probability that  $\hat{L}(\tau, h) = L$ .

**Theorem 1.** *Under Assumptions 1 and 2, for any  $\alpha > 0$ , there exists some  $\tau_{\alpha,h}$  such that the probability to overestimate the number of components is less than  $\alpha$ :*

$$\mathbb{P}(\hat{L}(\tau_{\alpha,h}) > L) < \alpha, \quad (9)$$

where

$$\tau_{\alpha,h} = \frac{1}{n^{1/2}} \left[ \frac{n+1}{n} C_{\alpha,1} \right]^{1/2} + \frac{1}{n^{1/2} h^d} C_2, \quad (10)$$

with  $C_{\alpha,1} = 36 \|K\|_2^{4d} \ln(1/\alpha) \mathbf{t}_{mix}$  and  $C_2 = \|K\|_2^{2d} (1 + 8\mathbf{t}_{mix})^{1/2}$ , and  $\mathbf{t}_{mix}$  is the mixing time of the underlying Markov chain recalled in Definition 2 in the Appendix.

If in addition Assumption 3 holds true and if  $h$  is small enough and  $n$  is large enough to ensure that for some  $\varepsilon > 0$ ,  $\sigma_L(T) > 2\tau_{\alpha,h} + \varepsilon$ , then

$$\mathbb{P}(\hat{L}(\tau_{\alpha,h}, h) < L) = 0 \text{ and } \mathbb{P}(\hat{L}(\tau_{\alpha,h}, h) = L) \geq 1 - \alpha. \quad (11)$$

From (9), the probability of overestimating the order of the HMM can be set as small as wanted for any value of the bandwidth  $h$ , and its related threshold is given by (10). Therefore, even if the singular values of  $T$  are estimated with bias from  $T_h$  (when  $h > 0$ ,  $\text{rank}(T) = \text{rank}(T_h) = L$  but for any  $j = 1, \dots, L$   $\sigma_j(T) \neq \sigma_j(T_h)$ ), we can make the probability of overestimating  $L$  as small as wanted if the sample size is large enough. This is no longer the case when dealing with the underestimation because  $\alpha$  and  $h$  should be defined in order to have  $\sigma_L(T) > 2\tau_{\alpha,h}$ . Thus, only the variance of the estimators  $\sigma_j(\hat{T}_{h,y})$  can lead to the overestimation of  $L$ . Indeed, despite the bias, the ranks of  $T$  and  $T_h$  are the same. However, both the bias and the variance of the estimators  $\sigma_j(\hat{T}_{h,y})$  impact the underestimation. Note that the condition  $\sigma_L(T) > 2\tau_{\alpha,h}$  cannot be verified in practice since it depends on the singular values of the theoretical operator. The following section gives rules on  $\alpha$  and  $h$  sufficient to ensure consistency of the estimator (9).

## 4.2 Asymptotic results

The following theorem states the consistency of the estimator of the number of states obtained by (7). We obtain the consistency by considering a suitable probability  $\alpha_n$  of overestimating the order and a suitable bandwidth  $h_n$  whose values depend on the sample size, without requiring consistency on the smallest non-zero singular value of  $T$ . The threshold  $\tau_{\alpha_n, h_n}$  depends on both the probability of overestimating the order and the bandwidth (see (10)). The quantities  $\alpha_n$  and  $h_n$  tend to zero when  $n$  tends to infinity. However, these quantities should tend to zero at an appropriate rate which ensures that  $\lim_{n \rightarrow \infty} r_{L+1}(\hat{T}_{h_n, \mathbf{y}})/\tau_{\alpha_n, h_n} = 0$  and  $\lim_{n \rightarrow \infty} \tau_{\alpha_n, h_n}/r_L(\hat{T}_{h_n, \mathbf{y}}) = 0$ . Indeed, considering  $\alpha_n$  tending to zero ensures that the order is not overestimating. However, to ensure that the order is not underestimated (see condition  $\sigma_L(T) > 2\tau_\alpha$  in Theorem 1), the threshold needs to tend to zero as the sample size tends to infinity.

**Theorem 2.** *Under Assumptions 1 and 2, if  $\ln(1/\alpha_n) = O(h_n^{2d})$  and  $h_n = n^{-\beta}$  where  $0 < \beta < 1/(2d)$ , then  $\hat{L}(\tau_{\alpha_n, h_n}, h_n)$  is a consistent estimator of  $L$  meaning that*

$$\lim_{n \rightarrow \infty} \mathbb{P}(\hat{L}(\tau_{\alpha_n, h_n}, h_n) = L) = 1. \quad (12)$$

## 5 Numerical experiments

This section starts by a comparison between the proposed method based on the integral operator and the spectral method of Lehéricy (2019), then it illustrates the relevance of the estimator (7) with numerical experiments on simulated and benchmark data. Results of (7) are obtained with  $\ln(1/\alpha_n) = 1/h_n^{2d}$ . For continuous data, a univariate Gaussian kernel with bandwidth  $h_n = \kappa n^{-\beta}$  is used while a univariate Von Mises kernel with bandwidth  $h_n = n^{-\beta}$  is used for circular data. In the case of univariate data (*i.e.*,  $d = 1$ ), the threshold is  $\tau_{\alpha_n, h_n} = n^{-1/2}h^{-1}$ , the bandwidth is defined with  $\beta = 1/6$  and  $\kappa = 0.9 \min(\text{var}^{1/2}(\mathbf{y}), \text{IQR}(\mathbf{y})/1.34)$  that corresponds to Silverman's rule (Silverman, 2018),  $\text{IQR}(\mathbf{y})$  being the empirical interquartile range. In the multivariate case, other constants are considered in such a way that the threshold is generalized by  $\tau_{\alpha_n, h_n} = n^{-1/2}h^{-d}10^{1-d}$  and the bandwidth is defined

with  $\beta = 1/(4 + 2d)$  and  $\kappa = 0.9 \prod_{j=1}^d \text{var}_j^{1/2}(\mathbf{y})$ , where  $\text{var}_j$  is the empirical variance of variable  $j$ . Note that the choice of  $\beta = 1/(4 + 2d)$  corresponds to the usual rate for kernel density estimation for random variables of dimension  $2d$ , which is explained by the fact that the density estimation fits the distribution of  $(\mathbf{Y}_t, \mathbf{Y}_{t+1})$ .

## 5.1 Comparing the operator-based method and the spectral method

Data are generated from an HMM defined with  $L = 3$  hidden states and transition matrix

$$A_\nu = \begin{bmatrix} 1 - 2\nu & \nu & \nu \\ \nu & 1 - 2\nu & \nu \\ \nu & \nu & 1 - 2\nu \end{bmatrix}.$$

Different distributions are considered for the emission distribution. First, observed data  $\mathbf{Y}_t$  are defined on  $[0, 1]$  since the emission distributions are Beta distributions such that  $\mathbf{Y}_t | X_t = 1 \sim \mathcal{B}(12, 1)$ ,  $\mathbf{Y}_t | X_t = 2 \sim \mathcal{B}(1, 12)$  and  $\mathbf{Y}_t | X_t = 3 \sim \mathcal{B}(12, 12)$ . Second, observed data  $\mathbf{Y}_t$  are defined on  $\mathbb{R}$  since the emission distributions are Gaussian distributions such that  $\mathbf{Y}_t | X_t = 1 \sim \mathcal{N}(-6, 1)$ ,  $\mathbf{Y}_t | X_t = 2 \sim \mathcal{N}(6, 1)$  and  $\mathbf{Y}_t | X_t = 3 \sim \mathcal{N}(0, 1)$ . Finally, we generated circular data since the emission distributions are Von Mises distributions such that  $\mathbf{Y}_t | X_t = 1 \sim \mathcal{VM}(\pi/2, 10)$ ,  $\mathbf{Y}_t | X_t = 2 \sim \mathcal{VM}(\pi/2 + 2\pi/3, 10)$  and  $\mathbf{Y}_t | X_t = 3 \sim \mathcal{VM}(\pi/2 + 4\pi/3, 10)$ . We compare the accuracy of integral-based method and the spectral method for recovering the true order  $L = 3$ . The spectral method estimates the order from the rank of the  $(M \times M)$  matrix  $\widehat{N}_M$  defined by  $\widehat{N}_M[k, \ell] = \frac{1}{n} \sum_{t=1}^n \phi_k(\mathbf{Y}_t) \phi_\ell(\mathbf{Y}_{t+1})$  where the functions  $\phi_1, \dots, \phi_M$  are basis functions. As suggested by Lehéricy (2019), the spectral method is used with trigonometric basis defined by  $\phi_0(\mathbf{Y}_t) = 1$  and  $\phi_k(\mathbf{Y}_t) = \sqrt{2} \cos(\pi k \mathbf{Y}_t)$  for  $k = 1, \dots, M$ . Note that for the case of Gaussian emission distributions, the observed sample is scaled as follows  $\tilde{\mathbf{Y}}_t = (\mathbf{Y}_t - \min_t \mathbf{Y}_t) / (\max_t \mathbf{Y}_t - \min_t \mathbf{Y}_t)$ . Moreover, a threshold must be applied on the observed singular values of  $\widehat{N}_M$ . As suggested in Section 5.3.2 of Lehéricy (2019), we consider an integer  $M_{\text{reg}} \leq M$  and we estimate the affine dependency of the singular values of  $\widehat{N}$  with respect to their index with a linear regression using its  $M_{\text{reg}}$  smallest singular values. Then, we set a thresholding parameter  $\tau = 1.5$  and we say that a

singular value is significant if it is above  $\tau$  times the value that the regression predicts for it. The estimator of the order is the number of consecutive significant singular values starting from the largest one. Thus, the spectral method has three tuning parameters: the basis family, the number of basis elements  $M$  (note that by construction, the estimator of the order is upper-bounded by  $M$ ) and the number  $M_{\text{reg}}$  of singular values used for determining the threshold.

Figure 1 presents the empirical probabilities that the competing methods select the true order of the HMM computed on 100 data sets generated with different sample sizes ( $n$ ) and different emission distributions. The spectral method is considered with  $M \in \{20, 40, 60\}$  and  $M_{\text{reg}} \in \{5, M/2, M - 5\}$ . Overall, the proposed method (see results of column integral operator in Figure 1) outperforms the spectral approach. Moreover, the spectral method seems to be sensitive to its tuning parameters.

The next section investigates the performances of the operator-based method on different setups. It illustrates the influence of the overlaps between the emission distributions, the influence of the mixing time, the influence of the bandwidth and the influence of the data dimension. Moreover, the computing time of the method is also investigated.

## 5.2 Investigating the operator-based method

**Simulation setup** Continuous data are generated from an HMM defined with  $L = 3$  hidden states and the transition matrix  $A_\nu$  defined in the previous experiment where the parameter  $\nu$  allows us to define different mixing times. Indeed, in the case where  $\nu = 1/3$ , this setup generates independent data, while the mixing time increases when  $\nu$  tends to zero. Conditionally on the hidden state  $X_t$ , the components of the vector  $\mathbf{Y}_t = (Y_{t1}, \dots, Y_{td})$  are independently generated from the model defined, for any  $t = 1, \dots, n+1$  and any  $j = 1, \dots, d$ , by

$$Y_{tj} = (\mathbf{1}_{\{X_t=2\}} - \mathbf{1}_{\{X_t=3\}}) \delta + \varepsilon_{tj},$$

where all  $\varepsilon_{tj}$  are generated independently and  $\delta$  is a constant tuning parameter. Different distributions are considered for  $\varepsilon_{tj}$  (Gaussian, Student with three degrees of freedom, Laplace

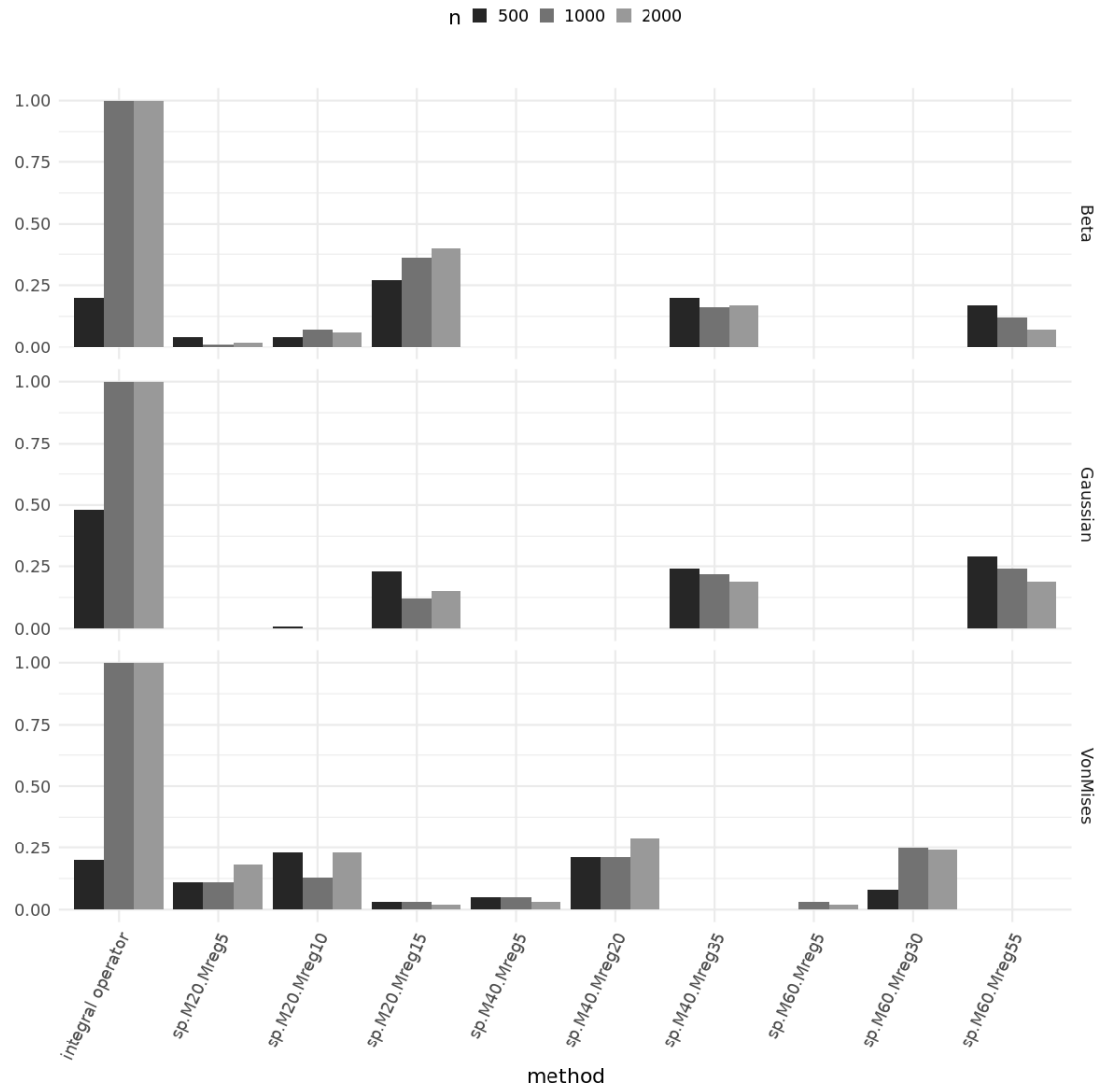


Figure 1: Empirical probabilities that the competing methods select the true order of the HMM computed on 100 data sets generated with  $\nu = 0.1$ , different sample sizes ( $n$ ) and different emission distributions.

and Exponential). The parameter  $\delta$  allows us to tune the overlaps between the emission distributions of each state.

**Influence of the overlap between emission distributions** To investigate the influence of the overlap between the emission distributions, data are generated with different values of  $\delta$ . Note that the higher the value of  $\delta$ , the more different the emission distributions are. Table 1 indicates the order estimated by (7) on 100 samples generated with  $d = 1$ ,  $\nu = 0.1$ , different sample sizes  $n$ , different families of emission distribution and different values of  $\delta$ . Overall, the results illustrate the consistency of the proposed estimator, as stated by Theorem 2. Indeed, for any family of distribution and any value of  $\delta$ , the estimator selects the true order with probability 1 when the sample size increases. Moreover, for small samples, the estimator does not overestimate the order but can underestimate it. Note that this phenomenon was already observed when the integral operator based approach proposed by Kwon and Mbakop (2021) is used for selecting the number of components in non-parametric mixture models. Finally, the more different the emission distribution, the more accurate the estimator for small samples.

**Influence of the mixing time** The mixing time appears in the constants  $C_{\alpha,1}$  and  $C_2$  that are in the definition of the threshold defined by (10). These constants increase with mixing time, and so decrease when  $\nu$  increases. The mixing time cannot be easily estimated, especially if the order is unknown. Consistency can be obtained for any value of the mixing time (see Theorem 2), which explains that we chose to neglect this constant (see definition of  $\tau_{\alpha_n, h_n}$  at the beginning of this section). However, we now investigate the influence of the mixing time on the accuracy of the resulting estimator by generating data with different  $\nu$ . Table 2 presents the order estimated by (7) on 100 samples generated with  $d = 1$ ,  $\delta = 5$ , different sample size, families of emission distribution and values of  $\nu$ . Again, the results illustrate the consistency of the approach. However, the results are deteriorated, for small samples, when  $\nu$  is close to the borders of its domain (*i.e.*, 0 or  $1/3$ ). Note that if  $\nu = 0$  or  $\nu = 1/3$ , then Assumption 1 does not hold. Indeed, when  $\nu$  tends to zero, then all the

$\delta$	$n$	Gaussian				Student				Laplace				Exponential			
		L-1	L-2	L-3	L>3	L-1	L-2	L-3	L>3	L-1	L-2	L-3	L>3	L-1	L-2	L-3	L>3
3	250	100	0	<b>0</b>	0	100	0	<b>0</b>	0	100	0	<b>0</b>	0	2	98	<b>0</b>	0
	500	20	80	<b>0</b>	0	92	8	<b>0</b>	0	77	23	<b>0</b>	0	0	20	<b>80</b>	0
	1000	0	99	<b>1</b>	0	0	100	<b>0</b>	0	0	100	<b>0</b>	0	0	0	<b>100</b>	0
	2000	0	1	<b>99</b>	0	0	100	<b>0</b>	0	0	100	<b>0</b>	0	0	0	<b>100</b>	0
	4000	0	0	<b>100</b>	0	0	3	<b>97</b>	0	0	0	<b>100</b>	0	0	0	<b>100</b>	0
4	250	78	22	<b>0</b>	0	99	1	<b>0</b>	0	99	1	<b>0</b>	0	2	97	<b>1</b>	0
	500	0	100	<b>0</b>	0	12	88	<b>0</b>	0	4	96	<b>0</b>	0	0	13	<b>87</b>	0
	1000	0	3	<b>97</b>	0	0	99	<b>1</b>	0	0	92	<b>8</b>	0	0	0	<b>100</b>	0
	2000	0	0	<b>100</b>	0	0	0	<b>100</b>	0	0	0	<b>100</b>	0	0	0	<b>100</b>	0
	4000	0	0	<b>100</b>	0	0	0	<b>100</b>	0	0	0	<b>100</b>	0	0	0	<b>100</b>	0
5	250	30	70	<b>0</b>	0	90	10	<b>0</b>	0	79	21	<b>0</b>	0	1	98	<b>1</b>	0
	500	0	89	<b>11</b>	0	0	100	<b>0</b>	0	0	100	<b>0</b>	0	0	8	<b>92</b>	0
	1000	0	0	<b>100</b>	0	0	26	<b>74</b>	0	0	5	<b>95</b>	0	0	0	<b>100</b>	0
	2000	0	0	<b>100</b>	0	0	0	<b>100</b>	0	0	0	<b>100</b>	0	0	0	<b>100</b>	0
	4000	0	0	<b>100</b>	0	0	0	<b>100</b>	0	0	0	<b>100</b>	0	0	0	<b>100</b>	0
6	250	12	88	<b>0</b>	0	60	40	<b>0</b>	0	43	57	<b>0</b>	0	1	98	<b>1</b>	0
	500	0	52	<b>48</b>	0	0	100	<b>0</b>	0	0	97	<b>3</b>	0	0	8	<b>92</b>	0
	1000	0	0	<b>100</b>	0	0	1	<b>99</b>	0	0	0	<b>100</b>	0	0	0	<b>100</b>	0
	2000	0	0	<b>100</b>	0	0	0	<b>100</b>	0	0	0	<b>100</b>	0	0	0	<b>100</b>	0
	4000	0	0	<b>100</b>	0	0	0	<b>100</b>	0	0	0	<b>100</b>	0	0	0	<b>100</b>	0

Table 1: Percentage of number of states selected by the estimator (7) computed on 100 replicates generated with  $d = 1$ ,  $\nu = 0.1$ , different families of the emission distributions, different overlaps of the emission distributions (tuned by  $\delta$ ) and different sample sizes  $n$ . Results related to the true order are in bold.

hidden states become absorbing states; while the transition matrix does not have full rank if  $\nu = 1/3$ , meaning that the model is not identifiable (in this case,  $\mathbf{Y}_t$  and  $\mathbf{Y}_{t'}$  are independent for  $t \neq t'$ ).

$\nu$	$n$	Gaussian				Student				Laplace				Exponential			
		L-1	L-2	L-3	L>3	L-1	L-2	L-3	L>3	L-1	L-2	L-3	L>3	L-1	L-2	L-3	L>3
0.01	250	35	65	<b>0</b>	0	47	53	<b>0</b>	0	44	56	<b>0</b>	0	21	70	<b>9</b>	0
	500	3	65	<b>32</b>	0	1	89	<b>10</b>	0	8	82	<b>10</b>	0	1	43	<b>56</b>	0
	1000	0	19	<b>81</b>	0	0	31	<b>69</b>	0	0	22	<b>78</b>	0	0	11	<b>89</b>	0
	2000	0	0	<b>100</b>	0	0	1	<b>99</b>	0	0	1	<b>99</b>	0	0	0	<b>100</b>	0
	4000	0	0	<b>100</b>	0	0	0	<b>100</b>	0	0	0	<b>100</b>	0	0	0	<b>100</b>	0
0.05	250	8	92	<b>0</b>	0	32	68	<b>0</b>	0	28	72	<b>0</b>	0	2	79	<b>19</b>	0
	500	0	47	<b>53</b>	0	0	100	<b>0</b>	0	0	96	<b>4</b>	0	0	8	<b>92</b>	0
	1000	0	0	<b>100</b>	0	0	3	<b>97</b>	0	0	1	<b>99</b>	0	0	0	<b>100</b>	0
	2000	0	0	<b>100</b>	0	0	0	<b>100</b>	0	0	0	<b>100</b>	0	0	0	<b>100</b>	0
	4000	0	0	<b>100</b>	0	0	0	<b>100</b>	0	0	0	<b>100</b>	0	0	0	<b>100</b>	0
0.10	250	30	70	<b>0</b>	0	90	10	<b>0</b>	0	79	21	<b>0</b>	0	1	98	<b>1</b>	0
	500	0	89	<b>11</b>	0	0	100	<b>0</b>	0	0	100	<b>0</b>	0	0	8	<b>92</b>	0
	1000	0	0	<b>100</b>	0	0	26	<b>74</b>	0	0	5	<b>95</b>	0	0	0	<b>100</b>	0
	2000	0	0	<b>100</b>	0	0	0	<b>100</b>	0	0	0	<b>100</b>	0	0	0	<b>100</b>	0
	4000	0	0	<b>100</b>	0	0	0	<b>100</b>	0	0	0	<b>100</b>	0	0	0	<b>100</b>	0
0.15	250	95	5	<b>0</b>	0	100	0	<b>0</b>	0	100	0	<b>0</b>	0	30	70	<b>0</b>	0
	500	0	100	<b>0</b>	0	39	61	<b>0</b>	0	16	84	<b>0</b>	0	0	66	<b>34</b>	0
	1000	0	17	<b>83</b>	0	0	98	<b>2</b>	0	0	93	<b>7</b>	0	0	0	<b>100</b>	0
	2000	0	0	<b>100</b>	0	0	0	<b>100</b>	0	0	0	<b>100</b>	0	0	0	<b>100</b>	0
	4000	0	0	<b>100</b>	0	0	0	<b>100</b>	0	0	0	<b>100</b>	0	0	0	<b>100</b>	0

Table 2: Percentage of number of states selected by the estimator (7) computed on 100 replicates generated with  $d = 1$ ,  $\delta = 5$ , different families of the emission distributions, different transition matrices (defined using  $\nu$ ) and different sample sizes  $n$ . Results related to the true order are in bold.

**Influence of the bandwidth** A range for the bandwidth ensuring consistency of (7) is stated in Theorem 2. Thus, we proposed to use a bandwidth of order  $n^{-1/(4+2d)}$  (see the beginning of this section) since this bandwidth allows the quadratic error between the true density and its kernel-based estimator to be minimized. Table 3 indicates the order estimated by (7) on 100 samples generated with  $d = 1$ ,  $\delta = 5$ ,  $\nu = 0.1$ , different sample

sizes, different families of emission distribution and different values of  $\beta$ . The estimator (7) is computed with a Gaussian kernel and a bandwidth  $h_n = \kappa n^{-\beta}$  defined with  $\kappa = 0.9 \min(\text{var}^{1/2}(\mathbf{y}), \text{IQR}(\mathbf{y})/1.34)$  and different values of  $\beta$ . In this simulation setup,  $\beta$  takes its values in  $\{1/4, 1/5, 1/6, 1/7\}$ , which all satisfy the condition of Theorem 2. For all the values of  $\beta$  considered in Table 3, the results illustrate the consistency of (7). However, for small samples, the proposed value (*i.e.*,  $\beta = 1/6$ ) provides the best results.

$\beta$	$n$	Gaussian				Student				Laplace				Exponential			
		L-1	L-2	L-3	L>3	L-1	L-2	L-3	L>3	L-1	L-2	L-3	L>3	L-1	L-2	L-3	L>3
1/4	250	82	18	<b>0</b>	0	100	0	<b>0</b>	0	100	0	<b>0</b>	0	2	97	<b>1</b>	0
	500	0	100	<b>0</b>	0	30	70	<b>0</b>	0	21	79	<b>0</b>	0	0	15	<b>85</b>	0
	1000	0	33	<b>67</b>	0	0	100	<b>0</b>	0	0	97	<b>3</b>	0	0	0	<b>100</b>	0
	2000	0	0	<b>100</b>	0	0	6	<b>94</b>	0	0	1	<b>99</b>	0	0	0	<b>100</b>	0
	4000	0	0	<b>100</b>	0	0	0	<b>100</b>	0	0	0	<b>100</b>	0	0	0	<b>100</b>	0
1/5	250	41	59	<b>0</b>	0	97	3	<b>0</b>	0	91	9	<b>0</b>	0	1	98	<b>1</b>	0
	500	0	92	<b>8</b>	0	1	99	<b>0</b>	0	0	100	<b>0</b>	0	0	11	<b>89</b>	0
	1000	0	0	<b>100</b>	0	0	48	<b>52</b>	0	0	25	<b>75</b>	0	0	0	<b>100</b>	0
	2000	0	0	<b>100</b>	0	0	0	<b>100</b>	0	0	0	<b>100</b>	0	0	0	<b>100</b>	0
	4000	0	0	<b>100</b>	0	0	0	<b>100</b>	0	0	0	<b>100</b>	0	0	0	<b>100</b>	0
1/6	250	30	70	<b>0</b>	0	90	10	<b>0</b>	0	79	21	<b>0</b>	0	1	98	<b>1</b>	0
	500	0	89	<b>11</b>	0	0	100	<b>0</b>	0	0	100	<b>0</b>	0	0	8	<b>92</b>	0
	1000	0	0	<b>100</b>	0	0	26	<b>74</b>	0	0	5	<b>95</b>	0	0	0	<b>100</b>	0
	2000	0	0	<b>100</b>	0	0	0	<b>100</b>	0	0	0	<b>100</b>	0	0	0	<b>100</b>	0
	4000	0	0	<b>100</b>	0	0	0	<b>100</b>	0	0	0	<b>100</b>	0	0	0	<b>100</b>	0
1/7	250	30	70	<b>0</b>	0	87	13	<b>0</b>	0	75	25	<b>0</b>	0	2	98	<b>0</b>	0
	500	0	94	<b>6</b>	0	0	100	<b>0</b>	0	0	100	<b>0</b>	0	0	11	<b>89</b>	0
	1000	0	0	<b>100</b>	0	0	33	<b>67</b>	0	0	7	<b>93</b>	0	0	0	<b>100</b>	0
	2000	0	0	<b>100</b>	0	0	0	<b>100</b>	0	0	0	<b>100</b>	0	0	0	<b>100</b>	0
	4000	0	0	<b>100</b>	0	0	0	<b>100</b>	0	0	0	<b>100</b>	0	0	0	<b>100</b>	0

Table 3: Percentage of number of states selected by the estimator (7) computed on 100 replicates generated with  $d = 1$ ,  $\delta = 5$ ,  $\nu = 0.1$ , different families of emission distributions, different bandwidths ( $h_n = \kappa n^{-\beta}$  with  $\kappa = 0.9 \min(\text{var}^{1/2}(\mathbf{y}), \text{IQR}(\mathbf{y})/1.34)$ ) and different sample sizes  $n$ . Results related to the true order are in bold.

**Influence of the data dimension** The proposed method allows us to handle multivariate data (*i.e.*, each  $\mathbf{Y}_t$  is a vector of dimension  $d$ ) for computing (7). Note that in this case,

we use  $\tau_{\alpha_n, h_n} = n^{-1/2} h^{-d} 10^{1-d}$  and the bandwidth is defined with  $\beta = 1/(4 + 2d)$  and  $\kappa = 0.9 \prod_{j=1}^d \text{var}_j^{1/2}(\mathbf{y})$ , where  $\text{var}_j$  is the empirical variance of variable  $j$ . Alternatively, as proposed by Kwon and Mbakop (2021), we could consider the maximum of the estimators computed from the marginal distribution of a single component of each  $\mathbf{Y}_t$ . This approach is justified since we have an upper-bound of the probability of overestimating the number of components. Table 4 presents the order estimated by (7) on 100 samples generated with  $\delta = 5$ ,  $\nu = 0.1$ , different sample sizes  $n$  and different dimensions  $d$ , for Gaussian emission distributions. The results illustrate the consistency of both the multivariate and the maximum of univariate methods. However, for small samples, the multivariate method is more accurate and the next paragraph shows that this method is less computationally intensive.

**Computing time** One strength of the proposed method is the ability to perform model selection without having to estimate the HMM parameters. Thus, for an application on real data, model selection is performed first then parameter estimation is done for the selected model. This allows setting an upper-bound of the number of states to be avoided. Moreover, since parameters are not fitted for all the competing models (as is done for penalized approach as in Lehéricy (2019)), the method should be computationally less intensive. To investigate the computational cost of the proposed method, Table 5 presents the mean of the computing time required for analyzing a single data set in the simulation setup considered to investigate the influence of the dimension. Results show that the proposed multivariate method is less computationally intensive. For such a method, the impact on the computing time of the dimension of  $\mathbf{Y}_t$  is slight. In addition, for moderate sample sizes the method is quite fast. However, as it requests the computation of a root-square of a  $(n + 1) \times (n + 1)$  matrix (see (6)), for data larger than  $10^4$  observations a way to compute quickly this matrix consists in using in this case the Adaptive Cross Approximate approach developed in Goreinov et al. (1997). This methods leads to approximate a matrix  $A \in \mathbb{R}^{n \times n}$  by a matrix of low rank by computing the CUR decomposition  $A \approx CUR$  where  $C \in \mathbb{R}^{n \times k}$  and  $R \in \mathbb{R}^{k \times n}$  are subsets of the columns and rows of  $A$  respectively, and  $U \in \mathbb{R}^{k \times k}$ .

dimension $d$	$n$	Multivariate-based estimator				Max. of univariate-based estimators			
		L-1	L-2	<b>L-3</b>	L>3	L-1	L-2	<b>L-3</b>	L>3
1	250	30	70	<b>0</b>	0	30	70	<b>0</b>	0
	500	0	89	<b>11</b>	0	0	89	<b>11</b>	0
	1000	0	0	<b>100</b>	0	0	0	<b>100</b>	0
	2000	0	0	<b>100</b>	0	0	0	<b>100</b>	0
	4000	0	0	<b>100</b>	0	0	0	<b>100</b>	0
2	250	0	93	<b>7</b>	0	21	79	<b>0</b>	0
	500	0	4	<b>96</b>	0	0	97	<b>3</b>	0
	1000	0	0	<b>100</b>	0	0	1	<b>99</b>	0
	2000	0	0	<b>100</b>	0	0	0	<b>100</b>	0
	4000	0	0	<b>100</b>	0	0	0	<b>100</b>	0
3	250	0	84	<b>16</b>	0	35	65	<b>0</b>	0
	500	0	1	<b>99</b>	0	0	100	<b>0</b>	0
	1000	0	0	<b>100</b>	0	0	0	<b>100</b>	0
	2000	0	0	<b>100</b>	0	0	0	<b>100</b>	0
	4000	0	0	<b>100</b>	0	0	0	<b>100</b>	0
4	250	4	94	<b>2</b>	0	40	60	<b>0</b>	0
	500	0	6	<b>94</b>	0	0	100	<b>0</b>	0
	1000	0	0	<b>100</b>	0	0	32	<b>68</b>	0
	2000	0	0	<b>100</b>	0	0	0	<b>100</b>	0
	4000	0	0	<b>100</b>	0	0	0	<b>100</b>	0

Table 4: Percentage of number of states selected by the multivariate-based estimator (7) and by the maximum of the estimators (7) obtained from single components of each  $\mathbf{Y}_t$  computed on 100 replicates generated with  $\delta = 5$ ,  $\nu = 0.1$ , Gaussian emission distributions, different sample sizes  $n$  and different dimension  $d$ . Results related to the true order are in bold.

dimension	$n$	Multivariate-based estimator	Max. of univariate-based estimators
$d$			
1	250	0	0
	500	3	3
	1000	25	25
	2000	188	189
	4000	1437	1443
2	250	0	1
	500	3	6
	1000	27	49
	2000	202	375
	4000	1524	2884
3	250	0	1
	500	3	9
	1000	31	73
	2000	259	564
	4000	1906	4340
4	250	0	2
	500	1	12
	1000	9	98
	2000	241	750
	4000	2337	5928

Table 5: Mean of the computing time, in seconds, required for assessing the multivariate-based estimator (7) and the maximum of the estimators (7) obtained from single components of each  $\mathbf{Y}_t$ , on a single sample generated with  $\delta = 5$ ,  $\nu = 0.1$ , Gaussian emission distributions, different sample sizes  $n$  and different dimension  $d$ .

### 5.3 Benchmark data

**Speed Accuracy Switching Data** This data set is composed of bivariate series  $\mathbf{Y}^{\{s\}} = (\mathbf{Y}_1^{\{s\}}, \dots, \mathbf{Y}_{n_s+1}^{\{s\}})$  describing length response times and accuracy scores of a single participant switching between slow/accurate responding and fast guessing on a lexical decision task (*i.e.*,  $\mathbf{Y}_t^{\{s\}} \in \mathbb{R} \times \{0, 1\}$ ). Three bivariate time series  $\mathbf{Y}^{\{1\}}$ ,  $\mathbf{Y}^{\{2\}}$  and  $\mathbf{Y}^{\{3\}}$  are available (*i.e.*,  $S = 3$ ) with lengths  $n_1 = 167$ ,  $n_2 = 133$  and  $n_3 = 136$ . Slow and accurate responding, and fast guessing can be modelled using two states, with a switching regime between them. Furthermore, the dataset contains a third variable called Pacc, representing the relative pay-off for accurate responding, which is on a scale of zero to one. This data set is from participant A in experiment 1.a. from Dutilh et al. (2011) and is available in the R package `depmixS4` (Visser and Speekenbrink, 2010). In this application, we focus on modeling the vector of response times. This vector is generally modeled by the same two-states HMM with Gaussian emission distributions for  $s = 1, \dots, S$ .

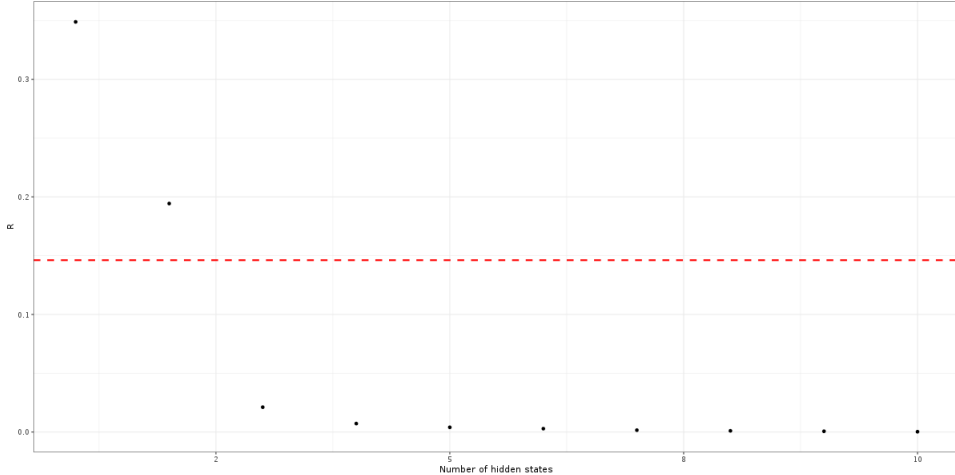


Figure 2: Values of  $r_{\ell}(\hat{T}_{h,y})$  (black dots) computed for the ten first hidden states (*i.e.*,  $\ell = 1, \dots, 10$ ) and threshold  $\tau$  (dashed line) obtained on the Speed Accuracy Switching data.

The choice of considering two states is justified by the fact that we want to model slow and fast answering. We propose using the estimator (7) for assessing the number of

hidden states without assuming Gaussian emission distributions. Considering that the three trials are independent, we extended the computation of the estimator (7) to data composed of  $S$  independent sequences of realizations drawn from the same HMM. To do this, we replace the kernel density estimator defined in (5) by  $\hat{p}_{h,y}(\mathbf{z}_1, \mathbf{z}_2) = (1/n) \sum_{s=1}^S \sum_{i=1}^n K_h^d(\mathbf{z}_1 - \mathbf{y}_t^{\{s\}}) K_h^d(\mathbf{z}_1 - \mathbf{y}_{t+1}^{\{s\}})$  where  $n = \sum_{s=1}^S n_s$ . The approach confirms the choice of two hidden states as shown by Figure 2. Indeed, this figure represents the values of  $r_\ell(\hat{T}_{h,y})$  computed for  $\ell = 1, \dots, 10$  as well as the value of the threshold. Therefore, the estimator (7) is defined as the number of dots which are above the dashed line. This figure shows a large gap between the values of  $r_2(T_{h,y})$  and  $r_3(T_{h,y})$ . Moreover, both  $r_2(T_{h,y})$  and  $r_3(T_{h,y})$  are not close to the threshold  $\tau$ . Therefore, the selection of  $L = 2$  is provided with high confidence.

Note that if an HMM with Gaussian emission distributions is used for modeling this data set, then the BIC selects three latent states. For this model, considering the most likely sequence of hidden states, we investigate the assumption of normality by performing the Shapiro-Wilk normality test per state, which provides the following  $p$ -values: 0.04389, 4.268e-06 and 9.449e-05. The assumption of normality can therefore be rejected. This could explain why the parametric approach with the BIC criterion detects three latent states while the proposed approach selects only two.

Figure 3 presents the recorded responses time, indicates the most-likely sequence of hidden states by gray-levels and shows the density estimators of the two emission distributions.

**Wind direction at Koeberg** South Africa's only nuclear power station is situated at Koeberg on the west coast, about 30 km north of Cape Town. The wind direction data consist of hourly values of average wind direction over the preceding hour at 35 m above ground level. The period covered is 1 May 1985 to 30 April 1989 inclusive. The average referred to is a vector average, which allows for the circular nature of the data, and is given in degrees. There are in total 35 064 observations with no missing values. The data are presented in Zucchini and MacDonald (2009) and are available from the book companion repository<sup>1</sup>. In

---

<sup>1</sup>file `wind2.txt` at <http://www.hmms-for-time-series.de/second/data/>

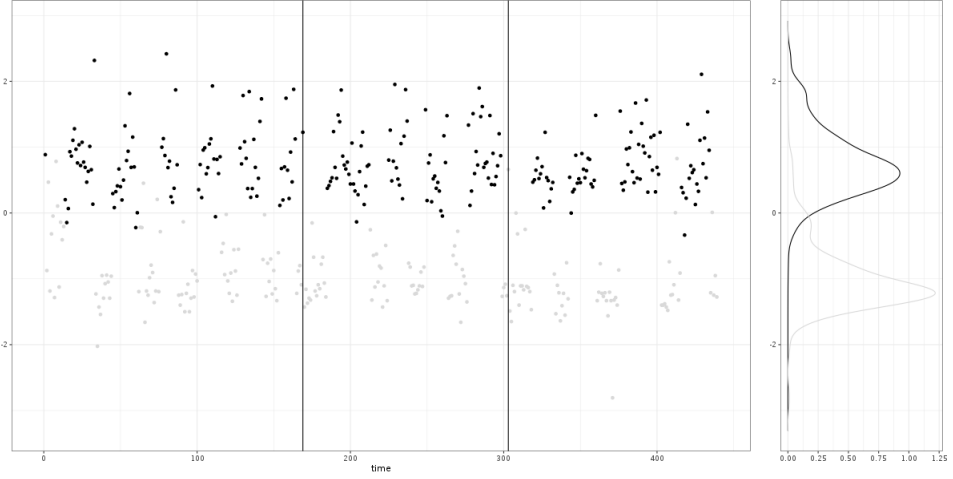


Figure 3: Responses time for participant A in experiment 1.a.. Colors indicate the most likely sequence of hidden states. The plot on the right side presents the kernel density estimators of the emission distributions. Vertical lines divide the three trials.

this application, we illustrate that the estimator (7) can be built on directional data (*i.e.*,  $\mathbf{Y}_t \in [0, 2\pi[$ ). We do this for the series of length 8766 formed by taking the directional data every 6 hours (*i.e.*, at hours 0, 6, 12 and 18 of each day). For directional data, the Gaussian kernel is not suitable and it can be replaced by the von-Mises kernel defined by  $K(u) = \exp(h^{-2} \cos u) / (2\pi I_0(h^{-2}))$  where  $I_k(v)$  denotes the modified Bessel function of the first kind with order  $k$  (see Hall et al. (1987)). Noting that the optimal bandwidth in the sense of the asymptotic mean integrated squared error obtained on  $q$ -dimensional directional data has a rate of  $n^{1/(4+q)}$ , we compute the estimator (7) with the von-Mises kernel with bandwidth  $h = n^{-1/6}$ . The estimator (7) selects three latent states as shown by Figure 4 that represents the values of  $r_\ell(\hat{T}_{h,y})$  computed for  $\ell = 1, \dots, 10$  as well as the value of the threshold. This figure shows that, despite the fact that the estimator selects three latent states, the statistics  $r_4(T_{h,y})$  is close to the threshold.

Figure 5 presenting the direction of the wind at Koeberg, indicates by gray-levels, the most-likely sequence of hidden states and shows the density estimators of the three emission distributions.

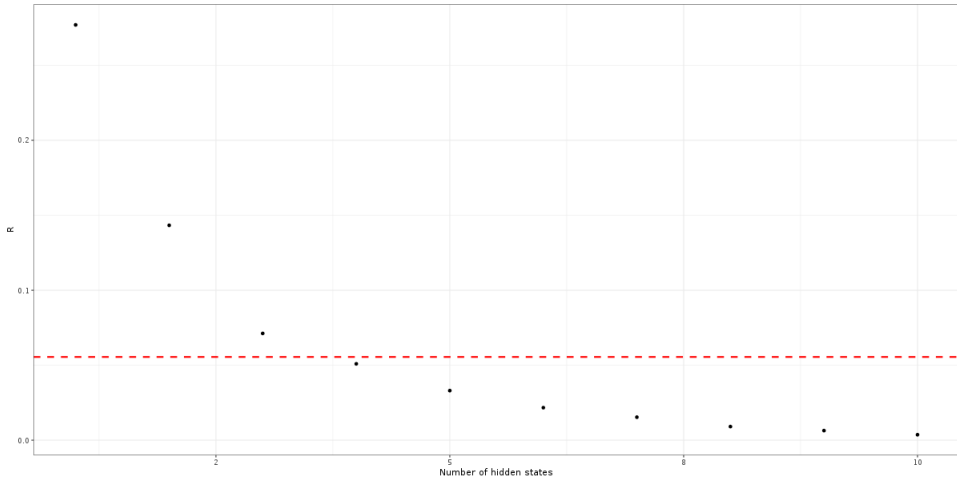


Figure 4: Values of  $r_\ell(\hat{T}_{h,y})$  (black dots) computed for the ten first hidden states (*i.e.*,  $\ell = 1, \dots, 10$ ) and threshold  $\tau$  (dashed line) obtained on the Wind direction at Koeberg data.

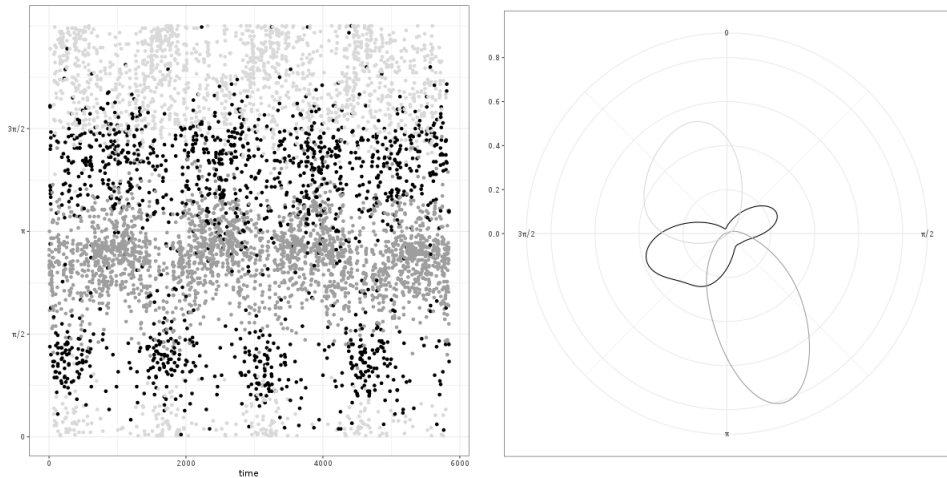


Figure 5: Direction of the wind at Koeberg record every six hours between May, 1st and April 30th 1989. Colors indicate the most likely sequence of hidden states. The plot on the right-hand side presents the kernel density estimators of the emission distributions.

## 6 Conclusion

In this paper, we introduced a new estimator for assessing the order of a non-parametric HMM by using the rank of an integral operator. To take into account the variability of the empirical singular values of a smoothed version of this operator, a data-driven thresholding rule is proposed. Under standard assumptions for non-parametric HMMs (*i.e.*, full rank covariance matrix and linear independence between the emission distributions), consistency of the estimator is established. As illustrated on benchmark data, the proposed approach considers different types of data including continuous data but also multivariate data or directional data. Numerical experiments illustrate that the proposed approach gives good results. However, as it involves the computation of the square root of matrices of size  $(n+1) \times (n+1)$ , the proposed approach is computationally intensive for very large samples. For large data sets (*i.e.*,  $n \geq 10^5$ ), alternative approaches approximating the root square of the matrix of interest could be used. For instance, the Adaptive Cross Approximate approach developed in Goreinov et al. (1997) could be considered. This methods leads to approximate a matrix  $A \in \mathbb{R}^{n \times n}$  by a matrix of low rank by computing the CUR decomposition  $A \approx CUR$  where  $C \in \mathbb{R}^{n \times k}$  and  $R \in \mathbb{R}^{k \times n}$  are subsets of the columns and rows of  $A$  respectively, and  $U \in \mathbb{R}^{k \times k}$ .

## References

Alexandrovich, G., Holzmann, H., and Leister, A. (2016). Nonparametric identification and maximum likelihood estimation for hidden markov models. *Biometrika*, 103(2):423–434.

Allman, E. S., Matias, C., and Rhodes, J. A. (2009). Identifiability of parameters in latent structure models with many observed variables. *The Annals of Statistics*, 37(6A):3099–3132.

Baum, L. E., Petrie, T., Soules, G., and Weiss, N. (1970). A maximization technique

occurring in the statistical analysis of probabilistic functions of markov chains. *The annals of mathematical statistics*, 41(1):164–171.

Benaglia, T., Chauveau, D., and Hunter, D. R. (2009). An em-like algorithm for semi- and nonparametric estimation in multivariate mixtures. *Journal of Computational and Graphical Statistics*, 18(2):505–526.

Bhatia, R. and Elsner, L. (1994). The hoffman-wielandt inequality in infinite dimensions. *Proceedings of the Indian Academy of Sciences - Mathematical Sciences*, 104(3):483–494.

Bickel, P. J., Ritov, Y., and Ryden, T. (1998). Asymptotic normality of the maximum-likelihood estimator for general hidden markov models. *The Annals of Statistics*, 26(4):1614–1635.

Bonhomme, S., Jochmans, K., and Robin, J.-M. (2016a). Estimating multivariate latent-structure models. *The Annals of Statistics*, 44(2):540–563.

Bonhomme, S., Jochmans, K., and Robin, J.-M. (2016b). Non-parametric estimation of finite mixtures from repeated measurements. *Journal of the Royal Statistical Society: Series B: Statistical Methodology*, pages 211–229.

Bulla, J., Lagona, F., Maruotti, A., and Picone, M. (2012). A multivariate hidden markov model for the identification of sea regimes from incomplete skewed and circular time series. *Journal of Agricultural, Biological, and Environmental Statistics*, 17(4):544–567.

Celeux, G. and Durand, J.-B. (2008). Selecting hidden markov model state number with cross-validated likelihood. *Computational Statistics*, 23(4):541–564.

Choo, K. H., Tong, J. C., and Zhang, L. (2004). Recent applications of hidden markov models in computational biology. *Genomics, proteomics & bioinformatics*, 2(2):84–96.

Chopin, N. (2007). Inference and model choice for sequentially ordered hidden markov models. *Journal of the Royal Statistical Society: Series B (Statistical Methodology)*, 69(2):269–284.

Ciuperca, G. (2002). Likelihood ratio statistic for exponential mixtures. *Annals of the Institute of Statistical Mathematics*, 54(3):585–594.

Couvreur, L. and Couvreur, C. (2000). Wavelet-based non-parametric hmm’s: theory and applications. In *2000 IEEE International Conference on Acoustics, Speech, and Signal Processing. Proceedings (Cat. No. 00CH37100)*, volume 1, pages 604–607. IEEE.

De Castro, Y., Gassiat, É., and Lacour, C. (2016). Minimax adaptive estimation of nonparametric hidden markov models. *The Journal of Machine Learning Research*, 17(1):3842–3884.

De Castro, Y., Gassiat, E., and Le Corff, S. (2017). Consistent estimation of the filtering and marginal smoothing distributions in nonparametric hidden markov models. *IEEE Transactions on Information Theory*, 63(8):4758–4777.

Du Roy de Chaumaray, M. and Marbac, M. (2021). Full model estimation for non-parametric multivariate finite mixture models. *arXiv preprint arXiv:2112.05684*.

Dutilh, G., Wagenmakers, E.-J., Visser, I., and van der Maas, H. L. (2011). A phase transition model for the speed-accuracy trade-off in response time experiments. *Cognitive Science*, 35(2):211–250.

Gassiat, E. and Boucheron, S. (2003). Optimal error exponents in hidden markov models order estimation. *IEEE Transactions on Information Theory*, 49(4):964–980.

Gassiat, É., Cleynen, A., and Robin, S. (2016). Inference in finite state space non parametric hidden markov models and applications. *Statistics and Computing*, 26(1):61–71.

Gassiat, E. and Keribin, C. (2000). The likelihood ratio test for the number of components in a mixture with markov regime. *ESAIM: Probability and Statistics*, 4:25–52.

Gassiat, E. and Rousseau, J. (2014). About the posterior distribution in hidden markov models with unknown number of states. *Bernoulli*, 20(4):2039–2075.

Gassiat, E. and Rousseau, J. (2016). Nonparametric finite translation hidden markov models and extensions. *Bernoulli*, 22(1):193–212.

Goreinov, S. A., Tyrtyshnikov, E. E., and Zamarashkin, N. L. (1997). A theory of pseudoskeleton approximations. *Linear algebra and its applications*, 261(1-3):1–21.

Hall, P., Watson, G., and Cabrera, J. (1987). Kernel density estimation with spherical data. *Biometrika*, 74(4):751–762.

Hansen, N. and Auger, A. (2011). Cma-es: evolution strategies and covariance matrix adaptation. In *Proceedings of the 13th annual conference companion on Genetic and evolutionary computation*, pages 991–1010.

Holzmann, H., Munk, A., Suster, M., and Zucchini, W. (2006). Hidden markov models for circular and linear-circular time series. *Environmental and Ecological Statistics*, 13(3):325–347.

Holzmann, H. and Schwaiger, F. (2016). Testing for the number of states in hidden markov models. *Computational Statistics & Data Analysis*, 100:318–330.

Hsu, D., Kakade, S. M., and Zhang, T. (2012). A spectral algorithm for learning hidden markov models. *Journal of Computer and System Sciences*, 78(5):1460–1480.

Hunter, D. R., Wang, S., and Hettmansperger, T. P. (2007). Inference for mixtures of symmetric distributions. *The Annals of Statistics*, pages 224–251.

Jin, N. and Mokhtarian, F. (2006). A non-parametric hmm learning method for shape dynamics with application to human motion recognition. In *18th International Conference on Pattern Recognition (ICPR'06)*, volume 2, pages 29–32. IEEE.

Juang, B. H. and Rabiner, L. R. (1991). Hidden markov models for speech recognition. *Technometrics*, 33(3):251–272.

Kasahara, H. and Shimotsu, K. (2014). Non-parametric identification and estimation of the number of components in multivariate mixtures. *Journal of the Royal Statistical Society: Series B (Statistical Methodology)*, 76(1):97–111.

Kleibergen, F. and Paap, R. (2006). Generalized reduced rank tests using the singular value decomposition. *Journal of econometrics*, 133(1):97–126.

Krogh, A., Larsson, B., Von Heijne, G., and Sonnhammer, E. L. (2001). Predicting transmembrane protein topology with a hidden markov model: application to complete genomes. *Journal of molecular biology*, 305(3):567–580.

Kwon, C. and Mbakop, E. (2021). Estimation of the number of components of nonparametric multivariate finite mixture models. *The Annals of Statistics*, 49(4):2178–2205.

Lambert, M. F., Whiting, J. P., and Metcalfe, A. V. (2003). A non-parametric hidden markov model for climate state identification. *Hydrology and earth system sciences*, 7(5):652–667.

Lehéricy, L. (2019). Consistent order estimation for nonparametric hidden markov models. *Bernoulli*, 25(1):464–498.

Leroux, B. G. (1992). Consistent estimation of a mixing distribution. *The Annals of Statistics*, pages 1350–1360.

Levine, M., Hunter, D. R., and Chauveau, D. (2011). Maximum smoothed likelihood for multivariate mixtures. *Biometrika*, 98(2):403–416.

Mastrantonio, G. and Calise, G. (2016). Hidden markov model for discrete circular–linear wind data time series. *Journal of Statistical Computation and Simulation*, 86(13):2611–2624.

Paulin, D. (2015). Concentration inequalities for markov chains by marton couplings and spectral methods. *Electronic Journal of Probability*, 20:1–32.

Petrie, T. (1969). Probabilistic functions of finite state markov chains. *The Annals of Mathematical Statistics*, 40(1):97–115.

Robert, C. P., Ryden, T., and Titterington, D. M. (2000). Bayesian inference in hidden markov models through the reversible jump markov chain monte carlo method. *Journal of the Royal Statistical Society: Series B (Statistical Methodology)*, 62(1):57–75.

Silverman, B. W. (2018). *Density estimation for statistics and data analysis*. Routledge.

Visser, I. and Speekenbrink, M. (2010). depmixs4: an r package for hidden markov models. *Journal of statistical Software*, 36:1–21.

Volant, S., Bérard, C., Martin-Magniette, M.-L., and Robin, S. (2014). Hidden markov models with mixtures as emission distributions. *Statistics and Computing*, 24(4):493–504.

Wolfer, G. and Kontorovich, A. (2019). Estimating the mixing time of ergodic markov chains. In *Conference on Learning Theory*, pages 3120–3159. PMLR.

Yang, L., Widjaja, B., and Prasad, R. (1995). Application of hidden markov models for signature verification. *Pattern recognition*, 28(2):161–170.

Yau, C., Papaspiliopoulos, O., Roberts, G. O., and Holmes, C. (2011). Bayesian non-parametric hidden markov models with applications in genomics. *Journal of the Royal Statistical Society: Series B (Statistical Methodology)*, 73(1):37–57.

Zhao, Z. (2011). Nonparametric model validations for hidden markov models with applications in financial econometrics. *Journal of econometrics*, 162(2):225–239.

Zucchini, W. and MacDonald, I. L. (2009). *Hidden Markov models for time series: an introduction using R*. Chapman and Hall/CRC.

## A Preliminary results

We recall here some definitions and basic properties of the mixing rate of Markov chains. We also provide some useful Lemmas, which will be proven in Appendix C.

In the following, we denote by  $(X_t)_{t \in \mathbb{Z}} \sim (A, \boldsymbol{\pi})$  a Markov chain with irreducible transition matrix  $A$  and stationary distribution  $\boldsymbol{\pi}$  and denote by  $\vec{X}_t$  the pair  $(X_t, X_{t+1})$ . First of all, we define the total variation distance between two probability distributions  $\mu$  and  $\nu$  on  $\{1, \dots, L\}$  by

$$\|\mu - \nu\|_{TV} = \frac{1}{2} \sum_{\ell \in \{1, \dots, L\}} |\mu(\ell) - \nu(\ell)|.$$

**Definition 1.** Let  $(X_t)_{t \in \mathbb{Z}} \sim (A, \boldsymbol{\pi})$  a Markov chain and define, for any  $t$ ,

$$d(t) = \sup_{\ell \in \{1, \dots, L\}} \|A^t(\ell, \cdot) - \boldsymbol{\pi}\|_{TV}.$$

The Markov chain is uniformly ergodic if  $d(t)$  goes to zero at a geometric rate as  $t$  goes to infinity, i.e. if there exists two constants  $c > 0$  and  $0 < \rho < 1$  such that  $d(t) \leq c\rho^t$ .

However, the constants supplied by Definition 1 are generally very difficult to calculate and too conservative to be of any practical use. Fortunately, we can do much better with the spectral gap and the mixing time. Hence, it is useful to introduce the mixing time variable which measures the time required by a Markov chain for the distance to stationarity to be small.

**Definition 2.** Let  $(X_t)_{t \in \mathbb{Z}} \sim (A, \boldsymbol{\pi})$ . Its mixing time  $t_{mix}$  is defined as

$$t_{mix} = \min\{t : d(t) \leq \frac{1}{4}\}.$$

It is well known that irreducible and aperiodic finite state chains are always uniformly ergodic and we can easily note that in this case,  $t_{mix}$  is finite and can be bounded by the (pseudo)-spectral gap of the transition matrix, see Wolfer and Kontorovich (2019).

First of all, we need to ensure that the hidden process  $\vec{\mathbf{Z}}_s = (\vec{X}_s, \vec{Y}_s)$  is a Markov chain with a mixing time that we are able to control, using the mixing time of the hidden Markov chain  $(X_t)_t$ .

**Lemma 4.** *Suppose that Assumption 1 holds true. Let  $X_1, \dots, X_n \sim (A, \boldsymbol{\pi})$  be a Markov chain with mixing time  $t_{mix}$  and stationary distribution  $\boldsymbol{\pi}$ . The hidden chain  $\vec{\mathbf{Z}} = (\vec{\mathbf{Z}}_1, \dots, \vec{\mathbf{Z}}_n)$  is also then a Markov chain with kernel transition  $A^{\vec{\mathbf{Z}}} : \{1, \dots, L\}^2 \times \mathbb{R}^{2d} \rightarrow [0, 1]$  and stationary distribution  $\boldsymbol{\pi}^{\vec{\mathbf{Z}}} = \boldsymbol{\pi}^{\vec{X}} \otimes G$  with  $G$  the transition kernel from  $\{1, \dots, L\}^2$  to  $\mathbb{R}^{2d}$  and  $\boldsymbol{\pi}^{\vec{X}}$  such that  $\boldsymbol{\pi}^{\vec{X}}(\ell, k) = \mathbb{P}_{\boldsymbol{\pi}}(X_s = \ell, X_{s+1} = k)$  for all  $(\ell, k) \in \{1, \dots, L\}^2$ . Furthermore, the mixing time of the Markov chain  $\vec{\mathbf{Z}}$  denoted  $t_{mix}^{\vec{\mathbf{Z}}}$  is at most  $t_{mix} + 1$ .*

**Lemma 5** (Covariance inequality for hidden Markov chains). *Suppose that Assumptions 1 and 2 hold true. Let  $X_1, \dots, X_n \sim (A, \boldsymbol{\pi})$  be a Markov chain with mixing time  $t_{mix}$  and stationary distribution  $\boldsymbol{\pi}$  and define the hidden Markov chain  $(\vec{\mathbf{Z}}_1, \dots, \vec{\mathbf{Z}}_n) \sim (A^{\vec{\mathbf{Z}}}, \boldsymbol{\pi}^{\vec{\mathbf{Z}}})$  from Lemma 4 with mixing time  $t_{mix}^{\vec{\mathbf{Z}}}$ . Then for any measurable function in  $L^2(\boldsymbol{\pi}^{\vec{\mathbf{Z}}})$ :  $\phi : \{1, \dots, L\}^2 \times \mathbb{R}^{2d} \rightarrow \mathbb{R}$ , we have*

$$\sum_{t=1}^n \mathbb{E}[\phi(\vec{\mathbf{Z}}_1)\phi(\vec{\mathbf{Z}}_t)] \leq 4t_{mix}^{\vec{\mathbf{Z}}} \mathbb{V}[\phi].$$

In particular, for  $\psi : \mathbb{R}^{2d} \rightarrow \mathbb{R}$  we have

$$\sum_{t=1}^n \mathbb{E}[\psi(\vec{Y}_1)\psi(\vec{Y}_t)] \leq 4t_{mix}^{\vec{\mathbf{Z}}} \mathbb{V}[\psi].$$

**Lemma 6** (Hoffman-Wielandt inequality (Bhatia and Elsner, 1994)). *Let  $\mathcal{T}$  and  $\mathcal{T}'$  be two operators with finite ranks, then we have that for any positive integer  $j$*

$$\sum_{i \geq j} (\sigma_i(\mathcal{T}) - \sigma_i(\mathcal{T}'))^2 \leq \|\mathcal{T} - \mathcal{T}'\|_{L^2(\mathbb{R}^d)}^2.$$

**Lemma 7.** *Under Assumptions 1 and 2, we have the following upper-bound, for any positive integer  $j$ ,*

$$|r_j(\hat{T}_{h,\mathbf{y}}) - r_j(T_h)| \leq \|\hat{T}_{h,\mathbf{y}} - T_h\|_{L^2(\mathbb{R}^d)},$$

where  $r_j$  is defined by (8).

**Lemma 8.** Let  $\phi : \mathbb{R}^d \times \mathbb{R}^d \rightarrow \mathbb{R}^+$  and  $\mathcal{T} : L^2(\mathbb{R}^d) \rightarrow L^2(\mathbb{R}^d)$  be the integral operator defined by

$$[\mathcal{T}(\omega)](\mathbf{z}_2) = \int_{\mathbb{R}^d} \omega(\mathbf{z}_1) \phi(\mathbf{z}_1, \mathbf{z}_2) d\mathbf{z}_1,$$

we have the following equivalence between the norms

$$\|\mathcal{T}\|_{L^2(\mathbb{R}^d)} = \|\phi\|_2,$$

where

$$\|\phi\|_2 = \left[ \int \phi^2(\mathbf{z}_1, \mathbf{z}_2) d\mathbf{z}_1 d\mathbf{z}_2 \right]^{1/2}.$$

**Lemma 9.** With the notations of Subsection 2.3 and Section 3, let  $g : \mathbb{R}^{d \times (n+1)} \rightarrow \mathbb{R}^+$  be given, for any  $\mathbf{Y} = (\mathbf{Y}_1, \dots, \mathbf{Y}_{n+1})$ , by

$$g(\mathbf{Y}) = \|\hat{p}_{h,\mathbf{Y}} - \mathbb{E}[K_h^d(\cdot - \mathbf{Y}_1)K_h^d(\cdot - \mathbf{Y}_2)]\|_2.$$

Then, under Assumption 2, for any  $\mathbf{y} \in \mathbb{R}^{d(n+1)}$  and  $\tilde{\mathbf{y}} \in \mathbb{R}^{d(n+1)}$ ,

$$|g(\mathbf{y}) - g(\tilde{\mathbf{y}})| \leq \frac{2\sqrt{2}}{n} \|K\|_2^{2d} \sum_{t=1}^{n+1} \mathbb{1}_{\{\mathbf{y}_t \neq \tilde{\mathbf{y}}_t\}}.$$

**Lemma 10.** Assume that Assumptions 1 and 2 are fulfilled. Then, for any  $h > 0$ , we have

$$\mathbb{E}[g(\mathbf{Y})] \leq \left( \frac{\|K\|_2^{4d}}{nh^{2d}} (1 + 8t_{mix}^{\vec{\mathbf{Z}}}) \right)^{1/2} \quad (13)$$

with  $t_{mix}^{\vec{\mathbf{Z}}}$  defined in Lemma 4 and  $g$  defined in Lemma 9.

**Lemma 11** (McDiarmid's inequality for Markov Chains (Paulin, 2015)). *1. Let  $\mathbf{V} = (V_1, \dots, V_n)^\top$*

*be a (not necessarily time homogeneous) Markov chain, taking values in a Polish state space  $\Lambda = \Lambda_1 \times \dots \times \Lambda_n$ . Suppose that  $g : \Lambda \rightarrow \mathbb{R}$  is such that there exists some  $\mathbf{c} = (c_1, \dots, c_n)$ , which satisfies that, for any  $\mathbf{v} \in \Lambda$  and  $\tilde{\mathbf{v}} \in \Lambda$ ,*

$$|g(\mathbf{v}) - g(\tilde{\mathbf{v}})| \leq \sum_{t=1}^n c_t \mathbb{1}_{\{v_t \neq \tilde{v}_t\}}.$$

Then for any  $t \geq 0$ , we have

$$\mathbb{P}(|g(\mathbf{V}) - \mathbb{E}g(\mathbf{V})| \geq t) \leq 2 \exp\left(\frac{-2t^2}{9\|\mathbf{c}\|^2 t_{mix}}\right),$$

where  $t_{mix}$  is the mixing time of the Markov chain defined in Lemma 4.

2. Let  $\mathbf{W} = (W_1, \dots, W_n)^\top$  be an hidden Markov chain with underlying chain  $\mathbf{V} = (V_1, \dots, V_n)^\top$  having mixing time  $t_{mix}$ . Suppose that  $g : \Lambda \rightarrow \mathbb{R}$  satisfies that for any  $\mathbf{w} \in \Lambda$  and  $\tilde{\mathbf{w}} \in \Lambda$

$$|g(\mathbf{w}) - g(\tilde{\mathbf{w}})| \leq \sum_{t=1}^n c_t \mathbb{1}_{\{w_t \neq \tilde{w}_t\}}, \quad (14)$$

for some  $\mathbf{c} = (c_1, \dots, c_n)$ , then for any  $t \geq 0$ , we have

$$\mathbb{P}(|g(\mathbf{W}) - \mathbb{E}g(\mathbf{W})| \geq t) \leq 2 \exp\left(\frac{-2t^2}{9\|\mathbf{c}\|^2 t_{mix}}\right),$$

## B Proofs of the main results

*Proof of Lemma 1.* Since, by Assumption 1.2, the densities  $\{f_1, \dots, f_L\}$  are linearly independent, there exist  $\kappa_1, \dots, \kappa_L$  with  $\kappa_\ell \in \mathbb{R}^d$  such that the  $L \times L$  matrix  $\mathbf{M}_f$  defined by  $\mathbf{M}_f[\ell, j] = f_\ell(\kappa_j)$ , has full rank. Let the  $L \times L$  matrix  $\mathbf{M}_g$  be defined by  $\mathbf{M}_g[\ell, j] = g_\ell(\kappa_j)$ . From (2), we have  $\mathbf{M}_g = \mathbf{A}\mathbf{M}_f$ . Noting that  $\det(\mathbf{M}_g) = \det(\mathbf{A})\det(\mathbf{M}_f)$  and that  $\mathbf{A}$  is invertible by Assumption 1.1, we have that  $\mathbf{M}_g$  has full rank and thus that the densities  $\{g_1, \dots, g_L\}$  are linearly independent. Thus, using Proposition 3 of Kasahara and Shimotsu (2014), we obtain that  $L$  is identifiable from the distribution of a pair of consecutive observations.  $\square$

*Proof of Lemma 2.* By Lemma 6, we have under Assumptions 1 and 2

$$\sum_{j=1}^L (\sigma_j(T_h) - \sigma_j(T))^2 \leq \|T_h - T\|_{L^2(\mathbb{R}^d)}^2. \quad (15)$$

Let  $G : \mathbb{R}^d \times \mathbb{R}^d \rightarrow \mathbb{R}$  be defined by  $G(\mathbf{z}_1, \mathbf{z}_2) = K^d(\mathbf{z}_1)K^d(\mathbf{z}_2)$ , where for any vector  $\mathbf{z} = (z_1, \dots, z_d)^\top \in \mathbb{R}^d$ ,  $K^d(\mathbf{z}) = \prod_{i=1}^d K(z_i)$ . For any bandwidth  $h > 0$ , let  $G_h$  be defined by  $G_h(\mathbf{z}_1, \mathbf{z}_2) = G(\mathbf{z}_1/h, \mathbf{z}_2/h)/(h^{2d})$ . Thus, we have  $G_h(\mathbf{z}_1, \mathbf{z}_2) = K_h^d(\mathbf{z}_1)K_h^d(\mathbf{z}_2)$  and since

$p_h(\mathbf{z}_1, \mathbf{z}_2) = \int_{\mathbb{R}^d \times \mathbb{R}^d} p(\mathbf{y}_1, \mathbf{y}_2) K_h^d(\mathbf{z}_1 - \mathbf{y}_1) K_h^d(\mathbf{z}_2 - \mathbf{y}_2) d\mathbf{y}_1 d\mathbf{y}_2$  we have  $p_h = p \star G_h$  where  $\star$  denotes the convolution product. Thus, variable change theorem implies that

$$p_h(\mathbf{z}_1, \mathbf{z}_2) = \int_{\mathbb{R}^d \times \mathbb{R}^d} p(\mathbf{z}_1 - \mathbf{u}_1 h, \mathbf{z}_2 - \mathbf{u}_2 h) G(\mathbf{u}_1, \mathbf{u}_2) d\mathbf{u}_1 d\mathbf{u}_2.$$

From Lemma 8, we have

$$\|T_h - T\|_{L^2(\mathbb{R}^d)}^2 = \int_{\mathbb{R}^d \times \mathbb{R}^d} \left[ \int_{\mathbb{R}^d \times \mathbb{R}^d} [p(\mathbf{z}_1 - \mathbf{u}_1 h, \mathbf{z}_2 - \mathbf{u}_2 h) - p(\mathbf{z}_1, \mathbf{z}_2)] G(\mathbf{u}_1, \mathbf{u}_2) d\mathbf{u}_1 d\mathbf{u}_2 \right]^2 d\mathbf{z}_1 d\mathbf{z}_2.$$

Therefore, a Taylor expansion of order 2 of  $p(\mathbf{z}_1 - \mathbf{u}_1 h, \mathbf{z}_2 - \mathbf{u}_2 h)$  around  $(\mathbf{z}_1^\top, \mathbf{z}_2^\top)^\top$  and Assumptions 3 implies that

$$\|T_h - T\|_{L^2(\mathbb{R}^d)}^2 = O(h^4). \quad (16)$$

□

Note that the proof of Lemma 3 is a modification of the proof of Corollary 3.1 in Kwon and Mbakop (2021).

*Proof of Lemma 3.* Let  $\hat{\mathcal{H}}_1$  and  $\hat{\mathcal{H}}_{n+1}$  be the random vector spaces defined respectively by

$$\hat{\mathcal{H}}_1 = \text{span}\{K_h^d(\cdot - \mathbf{Y}_t) | t = 2, \dots, n+1\} \text{ and } \hat{\mathcal{H}}_{n+1} = \text{span}\{K_h^d(\cdot - \mathbf{Y}_t) | t = 1, \dots, n\}.$$

Noting that the operator  $\hat{T}_{h,\mathbf{y}}$  can be rewritten as

$$[\hat{T}_{h,\mathbf{y}}(\omega)](\mathbf{z}_2) = \frac{1}{n} \sum_{t=1}^n K_h^d(\mathbf{z}_2 - \mathbf{Y}_{t+1}) \int_{\mathbb{R}^d} \omega(\mathbf{z}_1) K_h^d(\mathbf{z}_1 - \mathbf{Y}_t) d\mathbf{z}_1,$$

we have that the operator  $\hat{T}_{h,\mathbf{y}}$  has range in  $\hat{\mathcal{H}}_1$ . Note that all the  $\mathbf{Y}_t$ 's are distinct with probability 1. Thus, by Assumption 2, the vector spaces  $\hat{\mathcal{H}}_1$  and  $\hat{\mathcal{H}}_{n+1}$  have a dimension equal to  $n$  with probability 1 (see proof of Proposition 2.2 in Kwon and Mbakop (2021)).

Let the operators  $\Gamma_1 : \mathbb{R}^n \rightarrow \hat{\mathcal{H}}_1$  and  $\Gamma_n : \mathbb{R}^n \rightarrow \hat{\mathcal{H}}_{n+1}$  be defined by

$$\Gamma_1(\mathbf{a}) = \sum_{t=1}^n a_t K_h^d(\cdot - \mathbf{Y}_{t+1}) \text{ and } \Gamma_{n+1}(\mathbf{a}) = \sum_{t=1}^n a_t K_h^d(\cdot - \mathbf{Y}_t).$$

Note that for any  $\mathbf{a} \in \mathbb{R}^n$ ,

$$\|\Gamma_1(\mathbf{a})\|_{L^2(\mathbb{R}^d)}^2 = \mathbf{a}^\top \Delta_1^\top \hat{\mathbf{W}}_h \Delta_1 \mathbf{a} \text{ and } \|\Gamma_{n+1}(\mathbf{a})\|_{L^2(\mathbb{R}^d)}^2 = \mathbf{a}^\top \Delta_{n+1}^\top \hat{\mathbf{W}}_h \Delta_{n+1} \mathbf{a}.$$

Moreover,  $\widehat{\mathbf{W}}_h$  being symmetric definite positive (the functions  $K_h^d(\cdot - \mathbf{Y}_t)$  being linearly independent with probability one), the matrices  $\widehat{\mathbf{W}}_h^{1/2}$  and  $\widehat{\mathbf{W}}_h^{-1/2}$  are well defined. Thus, noting that

$$\Delta_1 \Delta_1^\top = \begin{bmatrix} 0 & \mathbf{0}_n^\top \\ \mathbf{0}_n & \mathbf{I}_n \end{bmatrix} \text{ and } \Delta_{n+1} \Delta_{n+1}^\top = \begin{bmatrix} \mathbf{I}_n & \mathbf{0}_n \\ \mathbf{0}_n^\top & 0 \end{bmatrix},$$

the matrices  $[\Delta_r^\top \widehat{\mathbf{W}}_h \Delta_r]^\alpha = \Delta_r^\top \widehat{\mathbf{W}}_h^\alpha \Delta_r$  are well defined for  $r \in \{1, n+1\}$  and  $\alpha \in \{-1/2, 1/2\}$ .

Therefore, we can define the operators  $R : \mathbb{R}^n \rightarrow \widehat{\mathcal{H}}_{n+1}$  and  $S : \widehat{\mathcal{H}}_1 \rightarrow \mathbb{R}^n$  by

$$R(\mathbf{a}) = \Gamma_{n+1}(\Delta_{n+1}^\top \widehat{\mathbf{W}}_h^{-1/2} \Delta_{n+1} \mathbf{a}) \text{ and } S(\Gamma_1(\mathbf{a})) = \Delta_1^\top \widehat{\mathbf{W}}_h^{1/2} \Delta_1 \mathbf{a}.$$

Note that the operators  $R$  and  $S$  are isometries. Indeed, using that, for  $r \in \{1, n+1\}$ ,  $\Delta_r^\top \widehat{\mathbf{W}}_h^{-1/2} \Delta_r \Delta_r^\top \widehat{\mathbf{W}}_h \Delta_r = \Delta_r^\top \widehat{\mathbf{W}}_h^{1/2} \Delta_r$ , we obtain that

$$\begin{aligned} \|R(\mathbf{a})\|_{L^2(\mathbb{R}^d)}^2 &= \|\Gamma_{n+1}(\Delta_{n+1}^\top \widehat{\mathbf{W}}_h^{-1/2} \Delta_{n+1} \mathbf{a})\|_{L^2(\mathbb{R}^d)}^2 \\ &= (\Delta_{n+1}^\top \widehat{\mathbf{W}}_h^{-1/2} \Delta_{n+1} \mathbf{a})^\top \Delta_{n+1}^\top \widehat{\mathbf{W}}_h \Delta_{n+1} (\Delta_{n+1}^\top \widehat{\mathbf{W}}_h^{-1/2} \Delta_{n+1} \mathbf{a}) \\ &= \|\mathbf{a}\|^2, \end{aligned}$$

and

$$\begin{aligned} \|S(\Gamma_1(\mathbf{a}))\|^2 &= (\Delta_1^\top \widehat{\mathbf{W}}_h^{1/2} \Delta_1 \mathbf{a})^\top \Delta_1^\top \widehat{\mathbf{W}}_h^{1/2} \Delta_1 \mathbf{a} \\ &= \|\Gamma_1(\mathbf{a})\|_{L^2(\mathbb{R}^d)}^2. \end{aligned}$$

Finally, we can deduce that

$$\hat{T}_{h,\mathbf{y}}(\Gamma_{n+1}(\mathbf{a})) = \frac{1}{n} \Gamma_1(\Delta_{n+1}^\top \widehat{\mathbf{W}}_h \Delta_{n+1} \mathbf{a}),$$

since for any  $\mathbf{z}_2 \in \mathbb{R}^d$

$$\begin{aligned} \frac{1}{n} \left[ \Gamma_1(\Delta_{n+1}^\top \widehat{\mathbf{W}}_h \Delta_{n+1} \mathbf{a}) \right] (\mathbf{z}_2) &= \frac{1}{n} \sum_{t=1}^n K_h^d(\mathbf{z}_2 - \mathbf{Y}_{t+1}) \sum_{s=1}^n \widehat{\mathbf{W}}_h[t, s] a_s \\ &= \frac{1}{n} \sum_{t=1}^n K_h^d(\mathbf{z}_2 - \mathbf{Y}_{t+1}) \int_{\mathbb{R}^d} K_h^d(\mathbf{z}_1 - \mathbf{Y}_t) \sum_{s=1}^n a_s K_h^d(\mathbf{z}_1 - \mathbf{Y}_s) d\mathbf{z}_1 \\ &= \frac{1}{n} \sum_{t=1}^n K_h^d(\mathbf{z}_2 - \mathbf{Y}_{t+1}) \int_{\mathbb{R}^d} K_h^d(\mathbf{z}_1 - \mathbf{Y}_t) [\Gamma_{n+1}(\mathbf{a})](\mathbf{z}_1) d\mathbf{z}_1 \\ &= \hat{T}_{h,\mathbf{y}}(\Gamma_{n+1}(\mathbf{a}))(\mathbf{z}_2). \end{aligned}$$

Let the operator  $\tilde{T}_h = S\hat{T}_{h,\mathbf{y}}R : \mathbb{R}^n \rightarrow \mathbb{R}^n$ . We now show that  $\tilde{T}_h$  and  $\hat{\mathbf{V}}_h$  have the same singular values. Indeed, for any  $\mathbf{a} \in \mathbb{R}^n$  and  $\mathbf{b} \in \mathbb{R}^n$ , we have

$$\begin{aligned}
\langle \mathbf{b}, \tilde{T}_h \mathbf{a} \rangle &= \langle \mathbf{b}, S\hat{T}_{h,\mathbf{y}}R\mathbf{a} \rangle \\
&= \langle \mathbf{b}, S\hat{T}_{h,\mathbf{y}}\Gamma_{n+1}(\Delta_{n+1}^\top \hat{\mathbf{W}}_h^{-1/2} \Delta_{n+1}\mathbf{a}) \rangle \\
&= \langle \mathbf{b}, \frac{1}{n}S\Gamma_1(\Delta_{n+1}^\top \hat{\mathbf{W}}_h \Delta_{n+1} \Delta_{n+1}^\top \hat{\mathbf{W}}_h^{-1/2} \Delta_{n+1}\mathbf{a}) \rangle \\
&= \langle \mathbf{b}, \frac{1}{n}S\Gamma_1(\Delta_{n+1}^\top \hat{\mathbf{W}}_h^{1/2} \Delta_{n+1}\mathbf{a}) \rangle \\
&= \langle \mathbf{b}, \frac{1}{n}\Delta_1^\top \hat{\mathbf{W}}_h^{1/2} \Delta_1 \Delta_{n+1}^\top \hat{\mathbf{W}}_h^{1/2} \Delta_{n+1}\mathbf{a} \rangle \\
&= \langle \mathbf{b}, \hat{\mathbf{V}}_h \mathbf{a} \rangle.
\end{aligned}$$

To conclude, it suffices to show that  $\tilde{T}_h$  and  $\hat{T}_{h,\mathbf{y}}$  have the same singular values. Using a singular value decomposition of  $\hat{T}_{h,\mathbf{y}}$ , we have

$$\hat{T}_{h,\mathbf{y}} = \sum_{j=1}^n \sigma_j(\hat{T}_{h,\mathbf{y}}) \hat{\nu}_j \otimes \hat{\mu}_j,$$

where  $\{\hat{\nu}_j\}_{j=1}^n$  and  $\{\hat{\mu}_j\}_{j=1}^n$  are two orthonormal basis. Noting that  $\tilde{T}_h = S\hat{T}_{h,\mathbf{y}}R$ , we have

$$\begin{aligned}
\tilde{T}_h &= S \left( \sum_{j=1}^n \sigma_j(\hat{T}_{h,\mathbf{y}}) \hat{\nu}_j \otimes \hat{\mu}_j \right) R \\
&= \sum_{j=1}^n \sigma_j(\hat{T}_{h,\mathbf{y}}) S\hat{\nu}_j \otimes R^\star \hat{\mu}_j,
\end{aligned}$$

where  $R^\star$  is the adjoint of  $R$ . Since  $R$  and  $S$  are isometries, the sets  $\{S\hat{\nu}_j\}_{j=1}^n$  and  $\{R^\star \hat{\mu}_j\}_{j=1}^n$  form two orthonormal basis. Therefore, the previous equation represents a singular value decomposition of  $\tilde{T}_h$  where the singular values are equal to the singular values of  $\hat{T}_{h,\mathbf{y}}$ .  $\square$

*Proof of Theorem 1.* By Lemma 7, applied with  $j = L + 1$ , we have, for any positive  $\tau$ , the following inclusion of events

$$\{\|\hat{T}_{h,\mathbf{y}} - T_h\|_{L^2(\mathbb{R}^d)} \leq \tau\} \subseteq \{|r_{L+1}(\hat{T}_{h,\mathbf{y}}) - r_{L+1}(T_h)| \leq \tau\},$$

which leads to this keystone inclusion

$$\{\|\hat{T}_{h,\mathbf{y}} - T_h\|_{L^2(\mathbb{R}^d)} \leq \tau\} \subseteq \{\hat{L}(\tau, h) \leq L\}. \quad (17)$$

Indeed, using the fact that  $T_h$  is of rank  $L$ , we have  $r_{L+1}(T_h) = 0$ , which implies that

$$\{\hat{L}(\tau, h) \leq L\} = \{r_{L+1}(\hat{T}_{h,\mathbf{y}}) \leq \tau\} = \{|r_{L+1}(\hat{T}_{h,\mathbf{y}}) - r_{L+1}(T_h)| \leq \tau\}.$$

Thus, controlling the probability that  $\hat{L}(\tau, h)$  overestimates  $L$  can be achieved via a concentration inequality on  $\|\hat{T}_{h,\mathbf{y}} - T_h\|_{L^2(\mathbb{R}^d)}$ . Noting that  $\mathbb{E}\hat{T}_{h,\mathbf{y}} = T_h$ , Lemma 8 implies

$$\|\hat{T}_{h,\mathbf{y}} - T_h\|_{L^2(\mathbb{R}^d)} = g(\mathbf{Y}),$$

with  $g : \mathbb{R}^{d \times (n+1)} \rightarrow \mathbb{R}^+$  and

$$g(\mathbf{Y}) = \|\hat{p}_{h,\mathbf{Y}} - \mathbb{E}[K_h^d(\cdot - \mathbf{Y}_1)K_h^d(\cdot - \mathbf{Y}_2)]\|_2.$$

Therefore, a concentration inequality on  $\|\hat{T}_{h,\mathbf{y}} - T_h\|_{L^2(\mathbb{R}^d)}$  can be obtained from a concentration inequality on  $g(\mathbf{Y})$ . From Lemma 9, we have for any  $\mathbf{y} \in \mathbb{R}^{d(n+1)}$  and  $\tilde{\mathbf{y}} \in \mathbb{R}^{d(n+1)}$ ,

$$|g(\mathbf{y}) - g(\tilde{\mathbf{y}})| \leq \frac{2\sqrt{2}}{n} \|K\|_2^{2d} \sum_{t=1}^{n+1} \mathbf{1}_{\{\mathbf{y}_t \neq \tilde{\mathbf{y}}_t\}}, \quad (18)$$

where  $\|K\|_2 = (\int_{\mathbb{R}} K(u)^2 du)^{1/2}$ . Thus, a concentration inequality on  $g(\mathbf{Y})$  can be achieved by a McDiarmid's inequality for Markov Chains (see Lemma 11) stated by Paulin (2015) since condition (14) is satisfied. Therefore, noting that vector  $c$  defined in Lemma 11 is here a vector of length  $n+1$  where each element is equal to  $2\sqrt{2}\|K\|_2^{2d}/n$ , we have for any  $t > 0$

$$\mathbb{P}(\|\hat{T}_{h,\mathbf{y}} - T_h\|_{L^2(\mathbb{R}^d)} \geq t + \mathbb{E}[g(\mathbf{Y})]) \leq \exp\left(-\frac{n^2}{n+1} \frac{t^2}{36\|K\|_2^{4d} t_{\text{mix}}}\right). \quad (19)$$

Moreover, from Lemma 10, we have

$$\mathbb{E}[g(\mathbf{Y})] \leq \left(\frac{\|K\|_2^{4d}}{nh^{2d}} \left(1 + 8t_{\text{mix}}\right)\right)^{1/2} \quad (20)$$

Therefore, replacing  $\mathbb{E}[g(\mathbf{Y})]$  by its upper-bound in (19), we have for any  $0 < \alpha < 1$

$$\mathbb{P}\left(\|\hat{T}_{h,\mathbf{y}} - T_h\|_{L^2(\mathbb{R}^d)} \geq [C_{1,\alpha}(n+1)/n^2]^{1/2} + \mathbb{E}[g(\mathbf{Y})]\right) \leq \alpha. \quad (21)$$

Combining (17) and (21) leads to (9).

In addition, to obtain (11), it is important to first notice the following equality of events

$$\{\hat{L}(\tau, h) = L\} = \left\{ \{r_L(\hat{T}_{h,\mathbf{y}}) > \tau\} \cap \{r_{L+1}(\hat{T}_{h,\mathbf{y}}) < \tau\} \right\}.$$

We then recall that  $r_{L+1}(T_h) = 0$  and that  $r_L(T_h) = \sigma_L(T_h)$ . Thus, by Lemma 7 applied with  $j = L + 1$  and  $j = L$  respectively, we obtain that

$$r_{L+1}(\hat{T}_{h,\mathbf{y}}) \leq \|\hat{T}_{h,\mathbf{y}} - T_h\|_{L^2(\mathbb{R}^d)},$$

and

$$r_L(\hat{T}_{h,\mathbf{y}}) \geq \sigma_L(T_h) - \|\hat{T}_{h,\mathbf{y}} - T_h\|_{L^2(\mathbb{R}^d)}.$$

Therefore, on the event  $\{\sigma_L(T_h) > 2\tau\} \cap \{\|\hat{T}_{h,\mathbf{y}} - T_h\|_{L^2(\mathbb{R}^d)} < \tau\}$ , we have  $r_{L+1}(\hat{T}_{h,\mathbf{y}}) < \tau$  and  $r_L(\hat{T}_{h,\mathbf{y}}) \geq \tau$ , which leads to the following inclusion of events

$$\left\{ \{\sigma_L(T_h) > 2\tau\} \cap \{\|\hat{T}_{h,\mathbf{y}} - T_h\|_{L^2(\mathbb{R}^d)} < \tau\} \right\} \subseteq \{\hat{L}(\tau, h) = L\}.$$

For any  $0 < \alpha < 1$ , the event  $\{\sigma_L(T_h) > 2\tau_\alpha\}$  is not random (see (10) for the definition of  $\tau_\alpha$ ). Thus, if there exists an  $\tilde{h}$  such that  $\sigma_L(T_{\tilde{h}}) > 2\tau_\alpha$ , we can then conclude that

$$\mathbb{P}(L(\tau_\alpha, \tilde{h}) = L) \geq 1 - \alpha.$$

To complete the proof, we have to show that such an  $\tilde{h}$  exists. Note that using Lemma 2 and the assumption that  $\sigma_L(T) > 2\tau_\alpha + \varepsilon$ , we obtain that

$$\sigma_L(T_h) > 2\tau_\alpha + \varepsilon + O(h^2),$$

which ensures the existence of  $\tilde{h}$ . □

## C Proofs of the preliminary lemmas

*Proof of Lemma 4.* Step 1: The Markov and stationary properties of the process  $\vec{\mathbf{X}} = (\vec{\mathbf{X}}_1, \dots, \vec{\mathbf{X}}_n)$  is straightforward. It remains just to prove that its mixing time is controlled

by the mixing time  $t_{mix}$  of the process  $(X_t)_{t \in \mathbb{Z}}$ . We denote by  $A^{\vec{X}} : \{1, \dots, L\}^2 \times \{1, \dots, L\}^2$  the kernel transition and by  $\pi^{\vec{X}}$  its stationary distribution, which are given for all  $(i, j, k, \ell) \in \{1, \dots, L\}^4$  by

$$A^{\vec{X}}((i, j), (k, \ell)) = \mathbf{1}_{\{k=j\}} A[k, \ell] \quad \text{and} \quad \pi^{\vec{X}}(i, j) = \mathbb{P}_{\pi}(X_s = i, X_{s+1} = j).$$

Let  $t \geq t_{mix} + 1$  and  $\delta_{(i_1, j_1)}$  the Dirac distribution on  $\{1, \dots, L\}^2$  that puts mass 1 at the pair  $(i_1, j_1)$  and 0 everywhere else, the total variation distance between  $(A^{\vec{X}})^t$  and the stationary distribution  $\pi^{\vec{X}}$  is then given by

$$\begin{aligned} \|\delta_{(i_1, j_1)}(A^{\vec{X}})^t - \pi^{\vec{X}}\|_{TV} &= \frac{1}{2} \sum_{(i, j) \in \{1, \dots, L\}^2} |\delta_{(i_1, j_1)}(A^{\vec{X}})^t[i, j] - \pi^{\vec{X}}(i, j)| \\ &= \frac{1}{2} \sum_{(i, j) \in \{1, \dots, L\}^2} |\mathbb{P}(\vec{X}_{t+1} = (i, j) | \vec{X}_1 = (i_1, j_1)) - A[i, j] \pi(i)| \\ &= \frac{1}{2} \sum_{(i, j) \in \{1, \dots, L\}^2} |\mathbb{P}((X_{t+1}, X_{t+2}) = (i, j) | (X_1, X_2) = (i_1, j_1)) - A[i, j] \pi(i)| \\ &= \frac{1}{2} \sum_{(i, j) \in \{1, \dots, L\}^2} |\mathbb{P}(X_{t+2} = j | X_{t+1} = i) \mathbb{P}(X_{t+1} = i | X_2 = j_1) - A[i, j] \pi(i)| \\ &= \frac{1}{2} \sum_{(i, j) \in \{1, \dots, L\}^2} |A[i, j] A^{t-1}[j_1, i] - A[i, j] \pi(i)| \\ &= \frac{1}{2} \sum_{i \in \{1, \dots, L\}} |A^{t-1}[j_1, i] - \pi(i)| \\ &= \|\delta_{j_1} A^{t-1} - \pi\|_{TV} \\ &\leq 1/4, \end{aligned}$$

where the last inequality is a consequence of Assumption 1 and the definition of the mixing time of  $(X_t)_t$ .

Step 2: : The Markov property and the mixing rate of the hidden state  $\vec{Z}$  is ensured from the stability properties of hidden chains, i.e. by taking the same strategy as in Step 1 for the Markov kernel  $A^{\vec{Z}}$  and let  $\delta_{(i_1, j_1, \tilde{y}_1, \tilde{y}_2)}$  the Dirac distribution on  $\{1, \dots, L\}^2 \times \mathbb{R}^{2d}$  that puts mass 1 at the pair  $(i_1, j_1, \tilde{y}_1, \tilde{y}_2)$  and 0 everywhere else, we have that

$$\|\delta_{(i_1, j_1, \tilde{\mathbf{y}}_1, \tilde{\mathbf{y}}_2)}(A^{\tilde{\mathbf{Z}}})^t - \boldsymbol{\pi}^{\tilde{\mathbf{Z}}}\|_{TV} = \|\delta_{(j_1, \tilde{y}_2)}(A^{X, \mathbf{Y}})^{t-1} - \boldsymbol{\pi}^{X, \mathbf{Y}}\|_{TV} \leq 1/4$$

where  $A^{X, \mathbf{Y}}$  is the Markov kernel transition of the hidden chain  $(X_t, \mathbf{Y}_t)$  and  $\boldsymbol{\pi}^{X, \mathbf{Y}}$  its stationary distribution which is also uniformly ergodic by stability and Assumption 1.  $\square$

*Proof of Lemma 5.* The proof is a direct consequence of Theorem 3.4 and Proposition 3.4 in Paulin (2015) for the hidden Markov chains  $\tilde{\mathbf{Z}} \sim (A^{\tilde{\mathbf{Z}}}, \boldsymbol{\pi}^{\tilde{\mathbf{Z}}})$  defined in Lemma 4 with mixing time  $t_{mix}^{\tilde{\mathbf{Z}}}$ . Taking for  $\phi$  the following function :

$$\phi : \begin{cases} \{1, \dots, L\}^2 \times \mathbb{R}^{2d} & \longrightarrow \mathbb{R} \\ (k, \ell, \tilde{\mathbf{y}}_1) & \longmapsto \psi(\tilde{\mathbf{y}}_1) \end{cases}$$

with  $\psi$  a measurable function from  $\mathbb{R}^{2d} \longrightarrow \mathbb{R}$ , we get

$$\sum_{t=1}^n \mathbb{E}[\psi(\tilde{\mathbf{Y}}_1)\psi(\tilde{\mathbf{Y}}_t)] \leq \frac{2}{\gamma_{ps}} \mathbb{V}[\psi]$$

where  $\gamma_{ps}$  is the pseudo-spectral gap associated with the kernel transition  $A^{\tilde{\mathbf{Z}}}$  (see Paulin (2015) for a definition). We conclude the proof by noting that, from Assumption 1, we have  $\frac{2}{\gamma_{ps}} \leq 4t_{mix}^{\tilde{\mathbf{Z}}}$ .  $\square$

*Proof of Lemma 7.* Using the reverse triangle inequality, we can easily show that, for any positive integer  $j$

$$|r_j(\hat{T}_{h, \mathbf{y}}) - r_j(T_h)| \leq \left[ \sum_{i \geq j} \left( \sigma_i(\hat{T}_{h, \mathbf{y}}) - \sigma_i(T_h) \right)^2 \right]^{1/2}.$$

We conclude the proof by using Lemma 6, which leads to the announced result

$$|r_j(\hat{T}_{h, \mathbf{y}}) - r_j(T_h)| \leq \|\hat{T}_{h, \mathbf{y}} - T_h\|_{L^2(\mathbb{R}^d)}.$$

$\square$

*Proof of Lemma 8.* Considering an orthonormal basis  $\{e_k\}_{k=1}^\infty$  of  $L^2(\mathbb{R}^d)$ , we have

$$\|\mathcal{T}\|_{L^2(\mathbb{R}^d)}^2 = \sum_{k=1}^\infty \int e_k(\mathbf{y}_1) \phi(\mathbf{y}_1, \mathbf{y}_2) d\mathbf{y}_2 d\mathbf{y}_1.$$

Therefore, denoting  $\phi_{\mathbf{y}_2} = \phi(\cdot, \mathbf{y}_2)$ , we have

$$\|\mathcal{T}\|_{L^2(\mathbb{R}^d)}^2 = \int \sum_{k=1}^\infty \langle \phi_{\mathbf{y}_2}, e_k \rangle d\mathbf{y}_2.$$

Applying Parseval's inequality we obtain

$$\|\mathcal{T}\|_{L^2(\mathbb{R}^d)}^2 = \int \|\phi_{\mathbf{y}_2}\|_2^2 d\mathbf{y}_2 = \|\phi\|_2^2,$$

which concludes the proof.  $\square$

*Proof of Lemma 9.* For any  $\mathbf{y} \in \mathbb{R}^{d(n+1)}$  and  $\tilde{\mathbf{y}} \in \mathbb{R}^{d(n+1)}$ , define  $\Delta = \{t : \mathbf{y}_t \neq \tilde{\mathbf{y}}_t\}$ . Let the vectors  $\mathbf{y}^{(s)}$  defined by  $\mathbf{y}^{(0)} = \mathbf{y}$  and for  $s = 1, \dots, \text{card}(\Delta)$  by

$$\mathbf{y}_t^{(s)} = \begin{cases} \mathbf{y}_t^{(s-1)} & \text{if } t \neq t^{(s)} \\ \tilde{\mathbf{y}}_t & \text{if } t = t^{(s)} \end{cases},$$

where  $t^{(s)}$  denotes the element  $s$  of  $\Delta$ . Applying the reverse triangle inequality, we have

$$|g(\mathbf{y}^{(s-1)}) - g(\mathbf{y}^{(s)})| \leq \|\hat{p}_{h, \mathbf{y}^{(s-1)}} - \hat{p}_{h, \mathbf{y}^{(s)}}\|_2.$$

Thus, if  $1 < t^{(s)} < n$ , we have

$$\begin{aligned} |g(\mathbf{y}^{(s-1)}) - g(\mathbf{y}^{(s)})| &\leq \frac{1}{n} \left[ \int K_h^d(\mathbf{z}_1 - \mathbf{y}_{t^{(s)}-1}^{(s-1)}) \left( K_h^d(\mathbf{z}_2 - \mathbf{y}_{t^{(s)}}^{(s-1)}) - K_h^d(\mathbf{z}_2 - \mathbf{y}_{t^{(s)}}^{(s)}) \right) \right. \\ &\quad \left. + \left( K_h^d(\mathbf{z}_1 - \mathbf{y}_{t^{(s)}}^{(s-1)}) - K_h^d(\mathbf{z}_1 - \mathbf{y}_{t^{(s)}}^{(s)}) \right) K_h^d(\mathbf{z}_2 - \mathbf{y}_{t^{(s)}+1}^{(s-1)}) d\mathbf{z}_1 d\mathbf{z}_2 \right]^{1/2}. \end{aligned}$$

Note that if  $t^{(s)} = 1$  or  $t^{(s)} = n$ , then the same reasoning can be applied but only one term appears in the integrand on the right-hand side of the previous equation. As  $K_h^d(\mathbf{z}_1 - \mathbf{y}_t) = \prod_{j=1}^d K((z_{1j} - y_{tj})/h)/h$  and as, by Assumption 2, we have  $\|K\|_2^2 = \int_{\mathbb{R}} K^2(u) du < \infty$ , we obtain that  $\int K_h^d(\mathbf{z}_1 - \mathbf{a}) K_h^d(\mathbf{z}_2 - \mathbf{b}) d\mathbf{z}_1 d\mathbf{z}_2 = \|K\|_2^{4d}$  for any  $\mathbf{a} \in \mathbb{R}^d$  and  $\mathbf{b} \in \mathbb{R}^d$ . Thus, using that  $(a+b)^2 \leq 4(a^2 \wedge b^2)$  and  $(a-b)^2 \leq 2(a^2 \wedge b^2)$  for any  $a > 0$  and  $b > 0$ , we deduce that

$$|g(\mathbf{y}^{(s-1)}) - g(\mathbf{y}^{(s)})| \leq \frac{2\sqrt{2}}{n} \|K\|_2^{2d}.$$

The proof is completed by noticing that  $\mathbf{y}^{(\text{card}(\Delta))} = \tilde{\mathbf{y}}$  and that

$$|g(\mathbf{y}) - g(\tilde{\mathbf{y}})| \leq \sum_{s=1}^{\text{card}(\Delta)} |g(\mathbf{y}^{(s-1)}) - g(\mathbf{y}^{(s)})|.$$

□

*Proof of Lemma 10.* Let us denote be  $U_{t,n}(\mathbf{z})$  the random variable defined as

$$U_{t,n}(\mathbf{z}) = K_h^d(\mathbf{z}_1 - \mathbf{Y}_t)K_h^d(\mathbf{z}_2 - \mathbf{Y}_{t+1})$$

where  $\mathbf{z} = (\mathbf{z}_1, \mathbf{z}_2)$ . We recall that the function  $g : \mathbb{R}^{d \times (n+1)} \rightarrow \mathbb{R}^+$  is such that

$$g(\mathbf{Y}) = \|\hat{p}_{h,\mathbf{Y}} - \mathbb{E}[K_h^d(\cdot - \mathbf{Y}_1)K_h^d(\cdot - \mathbf{Y}_2)]\|_2$$

with

$$\hat{p}_{h,\mathbf{y}}(\mathbf{z}) = \frac{1}{n} \sum_{t=1}^n K_h^d(\mathbf{z}_1 - \mathbf{y}_t)K_h^d(\mathbf{z}_2 - \mathbf{y}_{t+1}).$$

We also denote by  $p_h(\mathbf{z}) = \mathbb{E}[\hat{p}_{h,\mathbf{y}}(\mathbf{z})]$ . Hence, using the concavity of the square-root function and the Jensen's inequality, we get

$$\begin{aligned} \mathbb{E}[g(\mathbf{Y})] &= \mathbb{E} \left[ \left\| \frac{1}{n} \sum_{t=1}^n U_{t,n}(\mathbf{z}) - \mathbb{E}[U_{t,n}(\mathbf{z})] \right\|_2 \right] \\ &\leq \mathbb{E}^{1/2} \left[ \left\| \frac{1}{n} \sum_{t=1}^n (U_{t,n}(\mathbf{z}) - \mathbb{E}[U_{t,n}(\mathbf{z})]) \right\|_2^2 \right] \\ &\leq \mathbb{E}^{1/2} [\|\hat{p}_{h,\mathbf{y}}(\mathbf{z}) - p_h(\mathbf{z})\|_2^2] \end{aligned}$$

Using the standard bias variance decomposition, we obtain that

$$\begin{aligned}
\mathbb{E} [\|\hat{p}_{h,y}(\mathbf{z}) - p_h(\mathbf{z})\|_2^2] &= \mathbb{E} \left[ \int (\hat{p}_{h,y}(\mathbf{z}) - p_h(\mathbf{z}))^2 d\mathbf{z} \right] \\
&= \int \mathbb{E} [(\hat{p}_{h,y}(\mathbf{z}) - p_h(\mathbf{z}))^2] d\mathbf{z} \\
&= \int \mathbb{V}[\hat{p}_{h,y}] d\mathbf{z} \\
&= \int \mathbb{V} \left[ \frac{1}{n} \sum_{t=1}^n U_{t,n}(\mathbf{z}) \right] d\mathbf{z} \\
&= \int \left( \frac{1}{n^2} \sum_{t=1}^n \mathbb{V}[U_{t,n}(\mathbf{z})] + \frac{2}{n^2} \sum_{1 \leq t \leq t' \leq n} \text{Cov}(U_{t,n}(\mathbf{z}), U_{t',n}(\mathbf{z})) \right) d\mathbf{z} \\
&= \int \left( \frac{1}{n} \mathbb{V}[U_{1,n}(\mathbf{z})] + \frac{2}{n^2} \sum_{t=2}^n (n-t) \text{Cov}(U_{1,n}(\mathbf{z}), U_{t,n}(\mathbf{z})) \right) d\mathbf{z} \\
&\leq \int \left( \frac{1}{n} \mathbb{V}[U_{1,n}(\mathbf{z})] + \frac{2}{n} \sum_{t=2}^n \text{Cov}(U_{1,n}(\mathbf{z}), U_{t,n}(\mathbf{z})) \right) d\mathbf{z}
\end{aligned}$$

We start by computing the first term on the right-hand side

$$\begin{aligned}
\frac{1}{n} \int \mathbb{V}[U_{1,n}(\mathbf{z})] d\mathbf{z} &= \frac{1}{n} \int \mathbb{V} \left[ \frac{1}{h^{2d}} K^d \left( \frac{\mathbf{z}_1 - \mathbf{Y}_1}{h} \right) K^d \left( \frac{\mathbf{z}_2 - \mathbf{Y}_2}{h} \right) \right] d\mathbf{z} \\
&\leq \frac{1}{nh^{4d}} \int \left( \int \int K^{2d} \left( \frac{\mathbf{z}_1 - \mathbf{y}_1}{h} \right) K^{2d} \left( \frac{\mathbf{z}_2 - \mathbf{y}_2}{h} \right) p(\mathbf{y}_1, \mathbf{y}_2) d\mathbf{y}_1 d\mathbf{y}_2 \right) d\mathbf{z} \\
&\leq \frac{1}{nh^{2d}} \int \int \int K^{2d}(\mathbf{u}) K^{2d}(\mathbf{v}) p(\mathbf{z}_1 - \mathbf{u}h^d, \mathbf{z}_2 - \mathbf{v}h^d) d\mathbf{u} d\mathbf{v} d\mathbf{z} \\
&\leq \frac{1}{nh^{2d}} \|K\|_2^{4d}
\end{aligned} \tag{22}$$

Concerning the covariance terms, taking for  $\psi$ :

$$\psi : \begin{cases} \mathbb{R}^{2d} \longrightarrow \mathbb{R} \\ \vec{\mathbf{y}}_1 \longmapsto \psi(\vec{\mathbf{y}}_1) = K^d \left( \frac{\mathbf{z}_1 - \mathbf{y}_1}{h} \right) K^d \left( \frac{\mathbf{z}_2 - \mathbf{y}_2}{h} \right) \end{cases}$$

we have from Lemma 5

$$\begin{aligned}
& \sum_{t=2}^n Cov(U_{1,n}(\mathbf{z}), U_{t,n}(\mathbf{z})) \\
&= \frac{1}{h^{4d}} \sum_{t=2}^n Cov\left(K^d\left(\frac{\mathbf{z}_1 - \mathbf{Y}_1}{h}\right) K^d\left(\frac{\mathbf{z}_2 - \mathbf{Y}_2}{h}\right), K^d\left(\frac{\mathbf{z}_1 - \mathbf{Y}_t}{h}\right) K^d\left(\frac{\mathbf{z}_2 - \mathbf{Y}_{t+1}}{h}\right)\right) \\
&\leq \frac{1}{h^{4d}} \sum_{t=1}^n \left( \mathbb{E}\left[ \left| K^d\left(\frac{\mathbf{z}_1 - \mathbf{Y}_1}{h}\right) K^d\left(\frac{\mathbf{z}_2 - \mathbf{Y}_2}{h}\right) K^d\left(\frac{\mathbf{z}_1 - \mathbf{Y}_t}{h}\right) K^d\left(\frac{\mathbf{z}_2 - \mathbf{Y}_{t+1}}{h}\right) \right| \right] \right. \\
&\quad \left. + \left( \mathbb{E}\left[ \left| K^d\left(\frac{\mathbf{z}_1 - \mathbf{Y}_1}{h}\right) K^d\left(\frac{\mathbf{z}_2 - \mathbf{Y}_2}{h}\right) \right| \right] \right)^2 \right) \\
&\leq \frac{4t_{mix}^{\vec{\mathbf{Z}}}}{h^{4d}} \mathbb{V}\left[ K^d\left(\frac{\mathbf{z}_1 - \mathbf{Y}_1}{h}\right) K^d\left(\frac{\mathbf{z}_2 - \mathbf{Y}_2}{h}\right) \right] \\
&\leq \frac{4t_{mix}^{\vec{\mathbf{Z}}}}{h^{4d}} \mathbb{E}\left[ K^{2d}\left(\frac{\mathbf{z}_1 - \mathbf{Y}_1}{h}\right) K^{2d}\left(\frac{\mathbf{z}_2 - \mathbf{Y}_2}{h}\right) \right] \\
&\leq \frac{4t_{mix}^{\vec{\mathbf{Z}}}}{h^{4d}} \left( \int \int K^{2d}\left(\frac{\mathbf{z}_1 - \mathbf{y}_1}{h}\right) K^{2d}\left(\frac{\mathbf{z}_2 - \mathbf{y}_2}{h}\right) p(\mathbf{y}_1, \mathbf{y}_2) d\mathbf{y}_1 d\mathbf{y}_2 \right),
\end{aligned}$$

with  $t_{mix}^{\vec{\mathbf{Z}}}$  defined in Lemma 4. Integrating out the previous inequality over variable  $\mathbf{z}$ , we obtain that

$$\int \sum_{t=2}^n Cov(U_{1,n}(\mathbf{z}), U_{t,n}(\mathbf{z})) d\mathbf{z} \leq \frac{4t_{mix}^{\vec{\mathbf{Z}}} \|K\|_2^{4d}}{h^{2d}} \quad (23)$$

Combining (22) and (23), we obtain

$$\mathbb{E}[\|\hat{p}_{h,\mathbf{y}}(\mathbf{z}) - p_h(\mathbf{z})\|_2^2] \leq \frac{\|K\|_2^{4d}}{nh^{2d}} (1 + 8t_{mix}^{\vec{\mathbf{Z}}})$$

And, we can conclude with the announced bound

$$\mathbb{E}[g(\mathbf{Y})] \leq \left( \frac{\|K\|_2^{4d}}{nh^{2d}} (1 + 8t_{mix}^{\vec{\mathbf{Z}}}) \right)^{1/2}$$

□